Natural killer cells in the human lung tumor microenvironment display immune inhibitory functions

Jules Russick, Pierre-Emmanuel Joubert, Mélanie Gillard-Bocquet, Carine Torset, Maxime Meylan, Florent Petitprez, Marie-Agnès Dragon-Durey, Solenne Marmier, Aditi Varthaman, Nathalie Josseaume, et al.

Natural Killer cells in the human lung tumor microenvironment display immune inhibitory functions

Jules Russick[1]*, Pierre-Emmanuel Joubert[1]*, Mélanie Gillard-Bocquet[1]†, Carine Torset[1], Maxime Meylan[1], Florent Petitprez[2], Marie-Agnès Dragon-Durey[1,3], Solenne Marmier[1], Aditi Varthaman[1], Nathalie Josseaume[1], Claire Germain[1,††], Jérémy Goc[1], Marie-Caroline Dieu-Nosjean[4], Pierre Validire[5], Ludovic Fournel[6], Laurence Zitvogel[7,8], Gabriela Bindea[9], Audrey Lupo[1,6], Diane Damotte[1,6], Marco Alifano[1,6], Isabelle Cremer[1].

Affiliations

1. Centre de Recherche des Cordeliers, Sorbonne Universite, Inserm, Universite de Paris, Team Inflammation, complement and cancer, F-75006, Paris, France.

2. Programme Cartes d'Identité des Tumeurs, Ligue Nationale Contre le Cancer, Paris, France

3. Universite de Paris. Laboratoire d'immunologie, Hopital Europeen Georges Pompidou, APHP

4. Sorbonne Universite, INSERM U1135, Centre d'Immunologie et des Maladies Infectieuses, Team Immune Microenvironment and Immunotherapy, F-75013, Paris, France

5. Department of Pathology, Institut Mutualiste Montsouris, Paris, France

6. Departments of Pathology and Thoracic Surgery, Hospital Cochin Assistance Publique Hopitaux de Paris, F-75014 France

7. INSERM U1015, Gustave Roussy, 114 rue Edouard Vaillant, 94805, Villejuif Cedex, France

8. Universite Paris Saclay, Le Kremlin-Bicêtre, France

9. Centre de Recherche des Cordeliers, Sorbonne Universite, Inserm, Universite de Paris, Team Laboratory of Integrative cancer immunology, F-75006, Paris, France.

* Authors contributed equally to this work

† Current address : INSERM, U1212-ARNA, Institut Européen de Chimie et de Biologie, F-33607 Pessac, France

†† Current address : Invectys-Cancer Immunotherapeutics, Paris, France.

††† Current address : Joan and Sanford I. Weill Department of Medicine, Division of Gastroenterology and Hepatology, Department of Microbiology and Immunology and The Jill Robert's Institute for Research in Inflammatory Bowel Disease, Weill Cornell Medicine, Cornell University, New York, USA

Corresponding author:

Dr. Isabelle Cremer

Cordeliers Research Center, INSERM UMRS 1138

15 rue de l'Ecole de Medecine; 75006 Paris, France

Phone: 33-1-44-27-90-83/ Fax: 33-1-40-51-04-20

e-mail: isabelle.cremer@crc.jussieu.fr

Abstract

Backgroung: Natural Killer (NK) cells play a crucial role in tumor immunosurveillance through their cytotoxic effector functions and their capacity to interact with other immune cells to build a coordinated antitumor immune response. Emerging data reveal NK cell dysfunction within the tumor microenvironment through checkpoint inhibitory molecules associated with a regulatory phenotype.

Objective: We aimed at analyzing the gene expression profile of intratumoral NK cells compared to non-tumoral NK cells, and to characterize their inhibitory function in the tumor microenvironment.

Methods: NK cells were sorted from human lung tumor tissue and compared to non-tumoral distant lungs.

Results: In the current study, we identify a unique gene signature of NK cell dysfunction in human Non-Small-Cell Lung Carcinoma (NSCLC). First, transcriptomic analysis reveals significant changes related to migratory pattern with a down-regulation of *S1PR1* and *CX3CR1* and over-expression of *CXCR5* and *CXCR6*. Second, *CTLA4* and *KLRC1* inhibitory molecules were increased in intratumoral NK cells, and CTLA-4 blockade could partially restore MHC class II level on dendritic cell that was impaired during the dendritic cells (DC)/NK cell cross-talk. Finally, NK cell density impacts the positive prognostic value of $CD8^+$ T cells in Non-Small-Cell Lung Carcinoma.

Conclusions: These findings demonstrate novel molecular cues associated with NK cell inhibitory functions in NSCLC.

Key words

Natural killer cells, non small-cell lung carcinoma, antitumor immune surveillance, gene expression profile, CTLA-4, regulatory functions, clinical outcome, migration.

Background

Natural Killer (NK) cells are innate lymphoid cells (ILCs) representing the first line of defense against infected or transformed cells. They are highly cytotoxic, express many activating and inhibitory receptors and secrete cytokines and chemokines including TNF-α, IFN-γ, CCL3 and GM-CSF, allowing them to attract and interact with other immune cells(1).

In the tumor context, NK cell activation is tightly regulated by their interaction with malignant cells expressing various levels of NK receptor ligands. The current dogma is that NK cells act early in the anti-tumor immune response by controlling tumor burden and stimulating adaptive T cell immune responses(2) thereby curbing cancer cell metastasis(3). NK cells and T cells cooperate to restrain tumor growth, highlighting a role for NK cells in shaping adaptive anti-cancer responses. Indeed, patients with defective NK cell functions have been shown to have a higher incidence of cancers(4), while decreased peripheral blood NK cell activity is linked to increased carcinoma incidence(5).

Intratumoral NK cells display altered phenotype and functional impairment, relative to non-tumoral NK cells in patients with lung cancer(6,7), prostate cancer(8), breast cancer(9), hepatocellular carcinoma(10), and gastrointestinal stromal tumors(11). NK dysfunction has been attributed to direct crosstalk between tumor cells and NK cells, activated platelets and several soluble factors, such as myeloid derived suppressor cells (MDSCs), macrophage- and tumor cell-derived transforming growth factor β (TGF-β), prostaglandin E2, indoleamine-2,3-dioxygenase, adenosine, and interleukin-10 (IL-10)(4,7). In addition, loss of anti-tumor effects

in NK cells closely associated with aberrant fructose-1,6-biphosphatase (FBP1)-induced inhibition of glycolysis, and reduced NK cell viability(12). This can be explained by persistent stimulatory signaling and/or evading strategies used by tumor cells to escape NK cells, including the downregulation of important NK cell-activating ligands and/or an immunosuppressive tumor microenvironment (TME).

In Non-Small-Cell Lung Carcinoma (NSCLC), whereas tumor infiltrating $CD8^+$ T cells, $CD20^+$ B cells and DC-$LAMP^+$ mature dendritic cells (DC) strongly associate with a good clinical outcome(13–15), NK cell density is not linked to a prognostic value(7,16,17). This discrepancy can be explained by the fact that the TME is able to locally edit the phenotype of intratumoral NK cells, leading to reduced expression of activating receptors, increased expression of the inhibitory receptor natural killer group (NKG) 2A(7,18). NK cells may also acquire other immune checkpoint molecules(19,20) such as PD-1, LAG3, TIGIT, TIM3, CD73(21), and CIS(22) in certain tumor contexts. Preclinical studies show that NKG2A or TIGIT blockade enhances anti-tumor immunity mediated by NK cells(23–25), demonstrating the importance of targeting NK cells.

Microarray analysis of intratumoral, as compared to distant-lung tissue NK cells, reveal a specific transcriptional signature suggesting modulation of NK cell activity within the TME(26). However, the significance of this tumor-induced signature has not been investigated so far. Here we demonstrate, for the first time, that human NK cells express CTLA-4 in the lung, which is upregulated within the TME, and have a distinct expression of migratory receptors. Our data also show that CTLA-4-expressing NK cells have a negative impact on dendritic cells within the TME and impact the overall survival of $CD8^+$T cells in NSCLC patients.

Material and methods

Tissue samples from NSCLC patients

Human primary NSCLC samples and non-tumoral distant tissues (situated at more than 10 cm from the tumor) were obtained from non-treated patients the day of surgery at Institut Mutualiste Montsouris (Paris), Hotel-Dieu Hospital (Paris) or Cochin Hospital (Paris), from two prospective studies (Supplementary tables 1 and 4, respectively Cohort 1 discovery cohort, and Cohort 2 validation cohort). A retrospective NSCLC cohort was also used in this study (Cohort 3). Cohort 3 includes 539 untreated patients seen between 2001 and 2005 at the Department of Thoracic Surgery of Hotel-Dieu Hospital (Paris, France)(27). The inclusion criteria are histological subtypes squamous cell carcinoma (SCC) or lung adenocarcinoma (ADC), all TNM stages, and associated with clinical data. Histopathologic features such as histological subtypes, ADC grade, TNM stages are available for the majority of the patients.

All the patients gave an informed consent prior to inclusion. The study was conducted with the agreement of the French ethic committee (number 2012 06 12 IRB00001072) in application with the article L. 1121-1 of French law, according to the recommendations in the Helsinki declaration.

Preparation of human single-cell suspension

Surgical samples were mechanically dilacerated and single cell suspensions obtained after non-enzymatic disruption using the Cell Recovery Solution (Corning) for 1h at 4°C under agitation and filtered through a 70 µm cell strainer (BD Biosciences). Cells were washed in PBS+5%FCS+EDTA 0.5mM and mononuclear cells were purified using Lymphocyte Separation Medium gradient (Eurobio, Les Ulis, France). The number of cells obtained was then

134 determined by manual counting on Kova slides (Kova International, Garden Grove, CA, USA)
135 for further use.

136 **NK cell sorting**

137 Mononuclear cells were incubated with Live/Dead Fixable Yellow Dead Cell Stain Kit
138 (ThermoFischer, Waltham, MA, USA), PE-conjugated anti-CD45 (mIgG1κ, clone J.33, Beckman
139 Coulter), FITC conjugated anti-CD3 (BioLegend San Diego, CA, USA. mIgG1κ, clone UCHT1),
140 APC–conjugated anti-CD56 (BD Biosciences, Allschwil, Suisse, mIgG2bκ, clone N-CAM16.2) and
141 AF700-conjugated anti-CD11c (BD Biosciences, mIgG1κ, clone B-ly6) for 30 minutes at 4°C and
142 sorted with a FACS Aria III cell sorter (BD Biosciences). Sorted NK cells were defined as
143 $CD45^{+}CD3^{-}CD56^{+}$ cells, DC as $CD11c^{+}$ cells and purity after sorting was validated by flow
144 cytometry data using Diva software (BD Biosciences). For RNA analysis, sorted NK cells were
145 immediately collected in lysis buffer supplied in the RNA extraction kit (RNeasy Microkit –
146 Qiagen, MD, USA).

147 **Flow cytometry**

148 Cells were counted and stained using Live/Dead Fixable Yellow Dead Cell Stain Kit, CD45-PE or
149 FITC (Clone HI30, BioLegend), CD3-FITC (Clone UCHT1, ThermoFisher) or PerCP-Cy5.5 (Clone
150 SK7, BioLegend), CD56-APC or BV421 (Clone HCD56, BioLegend), NKp46-BV650 (9E2, BD
151 Biosciences), CX3CR1-APC (Clone 2A9-1, ThermoFisher), CD107a-APC-H7 (H4A3, BD
152 Biosciences), KLRC1-PE (Z199, Beckman Coulter), EOMES-Pe eFluor610 (Clone WD1928,
153 ThermoFisher), CXCR6-Pe-Cy7 (Clone SA051D1, BioLegend), BV450-conjugated anti-FoxP3
154 (Clone 259D/C7, BD Biosciences, mIgG1) and BV786-conjugated anti-CTLA-4 (Clone BNI3, BD
155 Biosciences, mIgG2aκ).

Antibodies and cells were incubated in PBS, 10% FCS, 0.5 mM EDTA Medium for 30' at 4°C and washed. Staining was acquired on Fortessa X20 (BD Biosciences) and analyzed using FlowJo software.

Microarray experiment and analysis

Microarray analysis was performed from previously described experiment(26).

RNA extraction from NK cells

Total RNA was extracted with the RNEasy Micro Kit (Qiagen) according to manufacturer's instructions. RNA quality and quantity were analyzed on a PicoChip (Total Eukaryote RNA Assay Pico II Kit; Qiagen) by capillary electrophoresis (BioAnalyzer; Agilent).

Reverse-Transcription and Preamplification

Reverse-transcriptions were performed on 5ng of total RNA in a 20µL reaction volume with the High Capacity cDNA Reverse Transcription Kit with RNAse inhibitor (PN 4368814; AppliedBiosystems™) according to the manufacturer's instructions.

12.5µL of cDNAs were pre-amplified with the Taqman® Preamp Master Mix Kit (AppliedBiosystems™) in a 50µL reaction volume containing 25µL of Master Mix 2× and 12.5µL of a pooled assay. Pooled assays combined equal volumes of each 20×Taqman® Gene Expression Assay of interest including the endogenous gene *CDKN1B* diluted using 1×TE buffer so that each assay is at a final concentration of 0.2×. A 14 cycles pre-amplification was performed, as recommended by the manufacturer and pre-amplification products were 1:20 diluted in 1×TE buffer.

Semi-quantitative real-time PCR

Semi-quantitative real-time PCR was performed with faststart universal probe master mix (Rox) 2× with 20×Taqman® Gene Expression Assay and 6.25µL of pre-amplified cDNA in a 25µL total reaction volume in each well of a 96-well plate. *CDKN1B* endogenous gene was used as recommended by the manufacturer in the preamp mastermix protocol. 7900HT Fast Real-Time PCR System (AppliedBiosystems™) was used for the detection and semi-quantification of gene expression.

TaqMan® Array Micro Fluidic Cards (Low-Density Arrays 384-wells format) were customized with our genes of interest and performed with FastStart Universal Probe Master Mix (Rox) 2× and pre-amplified cDNA in a 100µL total reaction volume on the 7900HT Fast Real-Time PCR System (AppliedBiosystems™).

Quantitative real-time PCR results were analyzed with the dedicated SDS2.3 and RQManager softwares (AppliedBiosystems™). For each probe and each sample, we normalized gene expression with the *CDKN1B* endogenous gene expression (ΔCt) and calculated the $\Delta\Delta$Ct and the corresponding fold-change ($2^{-\Delta\Delta Ct}$) between the Tum-NK and the Non-Tum-NK samples for each patient.

Immunohistochemistry

Tissues were deparaffinized and rehydrated by successive baths of Clearene and ethanol gradient (100%, 90%, 70%, 50%). Antigen retrieval was performed with a Tris-EDTA pH8 solution in a preheated water bath (97°C, 30 minutes). Sections were cooled at room temperature for 30 minutes and endogenous peroxidase was blocked with 3% hydrogen peroxide (15 minutes). Thereafter, sections were incubated with Protein Bock solution (Dako) for 30 minutes and incubated with mouse anti-human NKp46 (clone 195314, R&D Systems,

5µg/mL) and/or goat anti-human CTLA-4 mAb (AF-386-PB, R&D Systems, 2.5 µg/mL) for 1 hour at room temperature. Peroxidase-linked secondary antibody (ImmPress anti-goat HRP Vector) and alkaline phosphatase-linked secondary antibody (Rabbit anti-mouse AP Rockland Immunochemicals) were used for CTLA-4 and NKp46, respectively. AEC (3-amino-9-ethylcarbazole) and SAP (Shrimp-Alkaline Phosphatase) substrate (Vector laboratories) were used to detect specific staining. For immunofluorescence detection, PE-conjugated donkey anti-goat (Jackson ImmunoResearch) and AF647-conjugated donkey anti-mouse (Jackson ImmunoResearch) 1:100 diluted were used for CTLA-4 and NKp46, respectively. Mounting medium containing DAPI was used (Prolong Gold Antifade Mountant with DAPI, Invitrogen). Immunofluorescence was detected with AxioVert 200 microscope (Zeiss).

NKp46 quantification and image quantification (cohort 3)

NKp46 was stained by immunohistochemistry for 309 patients of the retrospective cohort (cohort 3). Slides were then digitalized using a NanoZoomer scanner (Hamamatsu Photonics. Hamamatsu, Japan) and NKp46 density was quantified (NK cell number per mm^2 tumoral tissue) with Calopix software (Tribun healthcare, France).

CD8 staining of NSCLC validation cohort (cohort 2) and image quantification

Serial 5-µm formalin-fixed paraffin-embedded NSCLC sections were stained using the Dako Autostainer Plus. Heat-mediated antigen retrieval was performed using the EnVision FLEX Target Retrieval Solutions (Agilent, Dako, CA. USA) at pH9 for 30 min on a PT-Link (Dako). Immunodetection of CD8 expression was done using a mouse anti-human CD8 antibody (Clone C8/144B. (Dako) at 1.6 µg/mL for 30 min in Dako REAL Antibody Diluent (Dako). Signal intensity was improved with EnVision+ System-HRP-labelled Polymers anti-mouse (Dako) and

peroxidase was detected using diaminobenzidine (DAB)+ Substrate – Chromogen System (Dako). Slides were then counterstained with Hematoxylin (Dako) and mounted with Glycergel Mounting Medium (Dako). Slides were then digitalized using a NanoZoomer scanner (Hamamatsu Photonics. Hamamatsu, Japan) and CD8 density was quantified with Halo software (Indica Labs NM, USA).

CD107a degranulation assay

Tumor infiltrating lymphocytes (TILs) from NSCLC patients were cultured for 12h in the presence of 100 U/ml IL-2 and incubated with K562 or P815 target cells at effector-target (E/T) ratios of 10:1 during 4 h, in the presence or not of anti-CD16 Ab, with monensin and PE Cy5-conjugated anti-CD107a (LAMP-1) mAb. Cells were then washed in PBS-FCS-EDTA and stained for 20 min at 4°C with FITC-conjugated anti-CD3 and APC-conjugated anti-CD56 or control conjugated isotypes.

Co-cultures of dendritic and NK cells

Tumor samples were processed as previously described (see "Preparation of human single-cell suspension"). NK cells and DC cells were sorted using Singlet/Live/$CD45^+$/$CD3^-$/$CD56^+$ and Singlet/Live/$CD45^+$/$CD11c^+$, respectively. Purity after cell isolation. The purity of cell subsets after cell sorting was assessed via flow cytometry prior to co-cultures and was between 94.6 to 100%, and between 98 to 99.6%, for NK cells and dendritic cells, respectively. Cells were then plated in a 96-well U bottom plate (30 to 50 x 10^3 cells/well) in RPMI 1640 Glutamax (ThermoFisher) supplemented with human serum (Sigma-Aldrich. St-Louis. MO. USA) and penicillin streptomycin (ThermoFisher) at 1:1 ratio of DC:NK. In the corresponding conditions, lipopolysaccharide (LPS-EB – InVivoGen, San Diego, CA, USA) and blocking anti-CTLA-4 antibody (ThermoFisher; clone AS32) were added at 1 μg/mL and at 5 μg/ml, respectively. DC

activation was assessed after 48h or 72h of co-culture by flow cytometry. Cells were stained using an APC Cy7-conjugated anti-HLA-DR (mIgG2aκ, clone L243, BioLegend) and an AF700-conjugated anti-CD86 (mIgG1κ, clone 2331, BD).

CTLA-4 and cytokine quantification produced by NK cells

Cell suspension from tumoral or non-tumoral tissues were obtained as described in "Preparation of human single-cell suspension**".** The cells were incubated overnight in a 96-well plate in in RPMI 1640 Glutamax supplemented with 10% human serum and 1% penicillin streptomycin, then the supernatant was kept at -80°C for CTLA-4 and cytokine dosages. Soluble CTLA-4 was quantified using ELISA Kit (Abcam) in the supernatant of cell cultures, following the manufacturer protocol. Cytokine production in the supernatant of cell cultures was evaluated using Luminex Assay (Bio-Plex Pro Human Cytokine 27-plex Assay - BioRad), following the manufacturer protocol.

Statistical and data analyses

Statistical analysis was performed using the R software version 3.6.0 and the packages pheatmap and ggplot2. Gene enrichment analysis was achieved with ClueGO(28) app of Cytoscape(29) with the Gene Ontology (GO) Biological processes database 2016 December. Association between quantitative and qualitative variables was estimated with Mann-Whitney U test. Association between quantitative variables was assessed using Pearson correlation. Association between qualitative variables was assessed using Fisher Test. A p-value <0.05 was considered statistically significant. The overall survival (OS) curves of patients with low *versus* high (separated by median) density of NKp46$^+$, CD8$^+$ T, DC-LAMP$^+$ DC or CD20$^+$ B cells, cells were estimated by the Kaplan–Meier method and compared by the log-rank test, and was performed using the script "*survfit*" on R studio software.

Results

NK cells in the tumor microenvironment display a distinct transcriptomic signature

To determine whether the gene expression signature of intratumoral NK cells is distinct in the lung TME, a whole transcriptome analysis was previously performed on purified NK cells from the tumor and matched distant tissue, in a discovery cohort of 12 NSCLC patients **(supplementary Table S1)**(26). In the present study, we performed a more extensive analysis of microarray data, and found a total of 968 genes differentially expressed between intratumoral NK cells and non-tumoral NK cells, with 569 over-expressed and 399 under-expressed genes, using the log2-fold change threshold of 1, with a p value inferior to 0.05 **(Figure 1A)** demonstrating that NK cells in the TME have a distinct transcriptomic signature. **Figure 1B** illustrates expression levels of these up and down regulated genes.

A gene ontology analysis using Cluego revealed that differentially expressed genes were involved in cell migration, regulation of response to stimulus, cell activation, defense response and inflammatory response **(Figure 1C)**, supporting major functional changes of NK cells within the TME. The under-expressed genes were associated with inflammatory response, endocytosis, response to inorganic substance, blood coagulation and hemostasis whereas the overexpressed ones were mainly associated with regulation of cell proliferation, cell activation and migration **(Figure 1D)**. Among the complete list of the 968 most differentially expressed genes **(Supplementary Tables S2 and S3),** those strongly linked to NK cell functions in the TME, i.e. migration, cell activation and regulation of immune responses and cytotoxicity, were selected to analyze their expression in a validation cohort of 47 NSCLC patients **(Supplementary Table S4)**.

The selected gene signature included *S1PR1*, *CX3CR1*, *CXCR5*, *CXCR6* and *CXCL13* (**Figure 2A**), *CTLA4*, *FCRL4*, *IL22RA2* and *LILRP2* (**Figure 2B**) and *FAS*, *GZMA*, *GZMK*, *NCR2* and *KLRC1* (**Figure 2C**). Semi-quantitative polymerase chain reaction (qRT-PCR) analysis performed on NK cells purified from tumor and matched non-tumor samples of the validation cohort confirmed the significant down-regulation of *S1PR1* and *CX3CR1*, and the over-expression of *CXCR5*, *CXCR6*, *CXCL13*, *CTLA4*, *FCRL4*, *IL22RA2*, *LILRP2*, *FAS*, *GZMA*, *GZMK*, *NCR2*, and *KLRC1* **(Figure 2A, B, C)**. Unsupervised hierarchical clustering of samples based on this gene expression signature resulted in segregation of non-tumoral and tumoral NK cells into distinct groups **(Figure 2D)**, confirming the modulation of NK cell migration, activation and cytotoxic functions in the TME. Unsupervised clustering based on expression variation of these genes in tumor NK cells compared to non-tumor NK cells revealed two groups of patients **(Figure 2E)**, with and an enrichment in migratory capacities in group 1 and in cytotoxic molecules in group 2**.** The two groups did not differ based on gender, tobacco, age, tumor size or presence of invaded lymph nodes **(Supplementary Fig. S1)**. However, we could notice an enrichment in stage 1 and 2 tumors and a trend for SCC histologic type enrichment in group 2 (**Supplementary Fig. S1)**.

A subset of intratumoral NK cells express CTLA-4

Although CTLA-4 is mainly expressed on regulatory T cells (Tregs) and some activated conventional T cell subsets (Tconv)(30) our analysis showed a strong upregulation of *CTLA4* mRNA in intratumoral NK cells in a subset of patients (77 %) **(Figure 2B)**. This expression was then validated at the protein level by immunohistochemistry and flow cytometry analyses. We observed the co-expression of CTLA-4 and NKp46 on intratumoral NK cells by immunohistochemistry and immunofluorescence on lung tumor tissue sections **(Figure 3A, B)**.

Of note, the expression of CTLA-4 by intratumoral NK cells was also observed in other solid tumors including melanoma, breast cancer and renal cell carcinoma **(Supplementary Fig. S2)**.

CTLA-4 expression was then compared by flow cytometry in NK, Tconv and Treg cells in several patients **(Figure 3C**). CTLA-4 expression in Tregs within the tumor as well as in distant lung non-tumoral tissue was confirmed both at the cell surface and intracellularly, whereas CTLA-4 was only expressed intracellularly by a fraction of NK and Tconv **(Figure 3D)**. In line with the results obtained by quantitative PCR, intracellular CTLA-4 was highly overexpressed in intratumoral NK cells in 11 out of 16 patients tested (69 %) **(Figure 3D)**. We therefore compared clinical data and survival of groups of patients with high and low CTLA-4$^+$ NK cells and found that there are significantly more patients with low CTLA-4$^+$ NK cells with adenocarcinoma histological type (75% vs 32%, p=0.02) and having stage I NSCLC (75% vs 40%, p= 0.07). We also found an influence of the gender since more female are found in the group of low CTLA-4$^+$ NK cells patients (81% vs 42%, p=0.01). Other clinical parameters were similar between patients with high and low CTLA-4$^+$ NK cells **(Supplementary Fig. S3A).** We also found no difference in the overall survival between the two groups of patients (**(Supplementary Fig. S3B).**

NK cells in the tumor microenvironment have a distinct phenotype and cytokine secretion profile

To better characterize the NK cells in the TME, we performed a flow cytometry analysis and quantified cytokine production by sorted NK cells. We first observed that among CD3$^-$CD56$^+$ NK cells, most of NKp46$^+$ cells co-express the transcription factor Eomes, which confirms that the cells belong to the NK lineage **(Figure 4A, B)**. We found a significant higher expression of NK2GA and CXCR6 and lower expression of CX3CR1 in NK cells from the TME as compared to

NK cells from non-tumoral tissue, confirming at the protein level the results obtained with gene expression analyses **(Figure 4A)**. Interestingly, we found that intratumoral NK cells display an activated phenotype, with high expression of CD69 and NKp44. However, no difference was found for Fas, CD107a and Eomes when we compared NK cells from TME or adjacent tissue **(Figure 4A)**. We also confirmed the co-expression of CTLA-4 and NKp46 by NK cells, and the co-expression of inhibitory CTLA-4 and NKG2A molecules on a subset of NK cells **(Figure 4B)**.

We found that NK cells from TME produced various levels of cytokines, with high levels of IL-1β, IL1RA, IL-6, IL-8, IL-9, IL-15, IL-17, TNF-α, IFN-γ and G-CSF and in similar amounts compared to NK cells from adjacent tissue **(Figure 4C)**.

Intratumoral NK cells has reduced cytotoxicity and negatively regulate dendritic cell maturation

We had previously demonstrated that intratumoral NK had reduced capacity to degranulate and to secrete IFN-γ after a coculture with autologous tumor cells(7). We also show that NK cells display reduced cytolytic function in a redirected lysis assay, against P815 mastocytoma cells **(Supplementary Fig. S4)**.

To analyze a possible regulatory role of intratumoral NK cells, we cocultured purified NK cells ($CD3^-CD56^+$) from fresh lung tumors and $CD11c^+$ dendritic cells (DC) purified from the blood of the same patients in the presence of LPS stimuli. When NK cell numbers permitted, we analyzed DC maturation in the presence of a blocking anti-CTLA-4 monoclonal antibody (mAb). After two to three days of coculture, DC maturation was assessed by flow cytometry **(Figure 5A, and gating strategy Supplementary Fig. S5)**. Induction of MHC class II and CD86 expression on DCs was significantly reduced upon coculture with intratumoral NK cells (20 and

41% inhibition, respectively) **(Figure 5B)**, and this was partially reverted by the addition of anti-CTLA-4 mAb **(Figure 5C)**. In addition, we didn't find any CTLA-4 protein in the supernatant of intratumoral NK cells (data not shown). These data suggest that intratumoral NK can reduce DC activation, through a mechanism that partially involves CTLA-4.

CTLA4 **expression by intratumoral NK cells is highly correlated with *CXCR6*, *GZMK* and *KLRC1***

To understand the suppressive effect of intratumoral NK cells on DC maturation, we evaluated the correlations between the expression of *CTLA4* and other genes in the signature. In tumors, we found an inverse correlation with *S1PR1*, and a strong positive correlation with *CXCR6*, *GZMK* and *KLRC1,* an inhibitory receptor on NK cells **(Figure 6)**. This suggests that *CTLA4*-expressing NK subsets may have a distinct migration and regulatory function profiles as compared with other NK cells.

Intratumoral NK cells negatively impact the clinical outcome of $CD8^+$ T cells

To investigate whether the presence of intratumoral NK cells could impact the clinical outcome, the localization and density of tumor-infiltrating NK cells were determined by NKp46 quantification on a retrospective cohort of NSCLC patients(27). IHC staining revealed that $NKp46^+$ cells were mainly localized in the stroma and poorly infiltrated the tumor nest **(Supplementary Fig. S6)**.

The prognostic value of intratumoral NK cells was determined using median cutoff separation of the groups. NK cell density was not linked to a prognosis in the entire cohort **(Figure 7A)**, in stage I and II **(Supplementary Fig. S7A),** tumor size **(Supplementary Fig. S7B)**, histological subgroups (**Supplementary Fig. S7C),** or chronic obstructive pulmonary disease (COPD) patients **(Supplementary Fig. S7D)**. Since some subsets of NK cells express inhibitory markers, including *KLRC1* and *CTLA4*, we hypothesized that the presence of inhibitory NK cells could

impact on the prognostic value of $CD8^+$ T cells. As previously reported, high $CD8^+$ T cell density strongly correlated to a good clinical outcome(14) **(Figure 7B)**. Consequently, the prognostic impact of NK cells differed when considering patient groups with high or low $CD8^+$ T cell infiltration. In patients with low numbers of $CD8^+$ T cells, high NK cell density improved the clinical outcome, whereas in patients with high $CD8^+$ T cell density, NK cells negatively impacted the overall survival **(Figure 7C)**, supporting the inhibitory role of intratumoral NK cells. This prognostic effect of NK cells is specific of T cells, since NK cell densities did not impact the clinical impact of B cells and mature DC-$LAMP^+$ dendritic cells **(Supplemental Figure S8).**

CTLA-4 expression by intratumoral NK cells is correlated to $CD8^+$ T cell density

Considering the expression pattern and suppressive role of CTLA-4 in tumor NK cells, we investigated the dynamics of *CTLA4* in tumor NK cells in the prospective cohort described in table 2 (cohort 2). We found a positive correlation between the density of $CD8^+$ T cells and the level of *CTLA4* gene expression by intratumoral NK cells **(Figure 7D)**, and a positive correlation between the percentage of CTLA-4^+ NK cells and the total percentage of $CD3^+$ T cells **(Supplementary Fig S9A)**. Finally, we also found a positive correlation between the gene expression level of *CTLA-4* and CD4 or CD8, both in adenocarcinoma and squamous cell carcinoma **(supplementary figure S9B)**, using gene expression profiling interactive analysis (GEPIA2) tool (http://gepia2.cancer.pku.cn/). Of note, total NK cell densities did not correlate with numbers of $CD8^+$ T cells, B cells or DCs **(Supplementary Table S5)**, suggesting that the possible inhibitory effect of NK cells was restricted to the subset of CTLA-4 expressing NK cells.

Discussion

In previous studies, we found that intratumoral NK cells exhibit altered phenotypes and functions(7) characterized by a specific gene expression signature(26). Here we extended this study with an in-depth transcriptomic analysis of NK cells in human NSCLC comparing the signature of intratumoral NK cells with distant non-tumoral lung NK cells. Our results show a distinct transcriptomic signature of NK cells in the lung TME suggesting that the lung TME may induce suppressive NK cells, that could play a role in the regulation of anti-tumor adaptive immunity.

Our signature is enriched with the chemokine receptors *CXCR5*, *CXCR6* and a show a strong downregulation of *S1PR1* and *CX3CR1*. The density of NK cells in the TME is lower than in distant tissue(7) and NK cells in the TME express more CXCR6 and less CX3CR1. This specific migratory signature could explain the exclusion of NK cells from the tumor core. Indeed, several studies show the involvement of CX3CR1 and fractalkine - the latter being expressed by tumor cells - in the recruitment and cytotoxicity of NK cells against tumors(31), and have shown TGF-β-mediated down-regulation of CX3CR1(32). In addition, CX3CR1-deficient mice have a defective anti-tumor response(33). On the other hand, a population of NK cells expressing CXCR6 is characterized by a more immature phenotype, producing fewer cytotoxic mediators and pro-inflammatory cytokines(34). The mechanism that explain this migratory profile found in intratumoral NK cells is unknown, but could be due to a preferential migration of cells that display this specific signature, to a local modification induced by the TME or a combination of both.

Intratumoral NK cells are also enriched with a number of inhibitory receptors most notable of which is CTLA-4, a well-known immune checkpoint molecule expressed by effector T cells after

426 TCR activation. It regulates T-cell activation by out-competing the co-stimulatory molecule
427 CD28 by binding its partners CD80 and CD86 with a higher avidity(30). However, data on the
428 expression and function of CTLA-4 in NK cells are scarce and poorly investigated. In studies by
429 Chiossone et al.(35) and Terme et al.(36), *CTLA4* transcripts were detected by whole-genome
430 microarray analysis of mouse NK cells, indicating that CTLA-4 may be expressed by NK cells. In
431 a recent study, CTLA-4 was found in $CD69^{+}CD103^{+}$ tissue resident NK cell subsets in human
432 lungs(37), and CTLA-4 expression is shown to be up-regulated in activated murine(38) and
433 human(39) NK cells. However, there is no evidence demonstrating CTLA-4 expression by NK
434 cells in the context of human lung tumors. We found that a subpopulation of intratumoral NK
435 cells have intracellular CTLA-4, as previously observed in a murine model of lung tumors,
436 showing CTLA-4 gene expression by intratumoral NK cells (38). Our immunohistochemistry
437 studies reveal that CTLA-4 is co-expressed with NKp46 also in other solid tumors suggesting
438 that its expression by NK cells is not restricted to lung tumors. Several isoforms of CTLA-4 have
439 been characterized(40). By RT-PCR, we found all the isoforms in NK cells purified from NSCLC
440 tumors (data not shown). Interestingly, *CTLA4* expression strongly correlated with that of
441 another inhibitory receptor *KLRC1*, specifically in the tumor tissue and co-expression of both
442 inhibitory receptors was confirmed in intratumoral NK cells, suggesting that, in the TME, NK
443 cells acquire inhibitory receptors making them less efficient effector cells.

444 The mechanism of action of CTLA-4 is still not completely clear. In co-culture experiments, we
445 found that tumor NK cells reduced DC maturation, and this was partially reversed by the
446 addition of CTLA-4 blocking antibodies. A possible effect of secreted CTLA-4 was excluded
447 since we did not detect soluble CTLA-4 in the NK cell supernatants. The precise mechanism of
448 this inhibition is unclear, but it could involve CTLA-4 -by maintaining its expression at the
449 surface level in the presence of the anti CTLA-4 Ab, as it has been suggested (41) - and other

yet unidentified molecules secreted or expressed by tumor-experienced NK cells, blocking the maturation or the recruitment of DC. Indeed, instances of NK cells suppressive DCs have been reported in previous studies: upregulation of PD-L1 on NK cells and PD-1 on DC led to impaired DC maturation and low $CD8^+$ T cell priming(42), while the impaired NK cell viability caused by tumor released PGE2 led to reduced recruitment of cDC1 in the TME(43).

While intratumoral NK cells exhibit altered functions, their density within the TME does not associate with improved clinical outcome, contrary to $CD8^+$ T cells that are linked to good overall survival (OS). Surprisingly, we found that high density of NK cells associates with a good OS only in patients with low infiltration of $CD8^+$ cells whereas it conferred a poor outcome in patients with high CD8 density. This highlights a role for the tumor immune microenvironment in re-programming NK cells. Accordingly, we found a positive correlation between higher $CD8^+$ T cell infiltration with CTLA-4 expression by NK cells suggesting that immune-active tumors also harbor suppressive NK cells. Of note, high NK cells density was also linked to good clinical outcome in COPD patients(27).

Despite the fact that NK cells have been widely implicated in anti-tumoral immune responses in various tumor models, several studies highlight their potential inhibitory/regulatory role. Regulatory NK cells produce IL-10 and/or express the immune checkpoint molecule CD73 and inhibit autologous $CD4^+$ T cell proliferation(21,44,45). Activated NK cells express granzyme K and NCR2(46,47) and kill autologous activated $CD4^+$ T cells by a mechanism involving granzyme K(48). We found that NK cells from the TME have a phenotype of activated cells - expressing CD69 and NCR2 molecules – and we found a strong correlation between *CTLA4* and *GZMK* expression, suggesting that tumor-experienced CTLA-4^+ NK cells could kill $CD4^+$ T cells. However, we did not find any decrease in T cell populations in tumors enriched in CTLA-4^+ NK

cells. The inhibitory function of intratumoral NK cells was also reported by Crome et al(49), who defined in high grade serous ovarian tumors a population of regulatory $CD56^{+}CD3^{-}$ cells that suppressed TIL expansion, displayed low cytotoxic activity and produced IL-9 and IL-22 cytokines. This population resembles partially the one we describe in our study, based on cytokine profile and phenotypic characteristics. Finally, in advanced NSCLC, a regulatory role of NKp46+ NK cells has been reported, showing that low rates of circulating $NKp46^{+}$ NK cells significantly associated with better OS(50).

Conclusions

Our findings on the regulatory function of NK cells in the lung TME have several therapeutic implications. First, the characterization of intratumoral NK cells reveals a specific migration profile potentially restricting their entry into the TME. It would be of great interest to target chemokine receptors on NK cells to enable them to enter tumor tissues. Second, our results show that NK cells acquire inhibitory functions within the TME, the reversion of which will enable NK cells to activate other immune cells and exert anti-tumoral cytotoxic functions. During the past 10 years, antibodies targeting CTLA-4 and PD1/ PD-L1, have entered clinical trials to reverse T cell exhaustion and restore the anti-tumor capacity of T cells, with proven efficacy in patients with various types of advanced cancers, including NSCLC(51). In addition, several clinical trials based on NK cell checkpoints are ongoing, targeting KIR, TIGIT, LAG-3, TIM-3 and KLRC1(19). In this context, both $CD8^{+}$ T cells and NK cells have been shown necessary for the therapeutic effectiveness of combination IL-2 and CTLA-4 blockade immunotherapy in B16 melanoma(52). Our study provides data supporting the pertinence of targeting the inhibitory activity of NK cells within the TME.

In conclusion, our results support the notion that the TME contains regulatory NK cells, that

represents a new escape mechanism.

List of abbreviations

CCL3 : C-C Motif Chemokine Ligand 3

cDC1 : conventional dendritic cell 1

CIS : cytokine-inducible SH2-containing protein

COPD : chronic obstructive pulmonary disease

CTLA-4 : cytotoxic T-lymphocyte-associated protein 4

CX3CR1 : CX3C chemokine receptor 1

CXCL13 : C-X-C motif ligand 13

CXCR5 : C-X-C chemokine receptor type 5

CXCR6 : C-X-C chemokine receptor type 6

FAS : FS7-associated cell surface antigen

FCRL4 : Fc receptor-like protein 4

GM-CSF : Granulocyte Macrophage Colony-Stimulating Factor

GZMA : Granzyme A-encoding gene

GZMK : Granzyme K-encoding gene

IL22RA2 : Interleukin 22 Receptor Subunit Alpha 2

KLRC1 : Killer Cell Lectin Like Receptor C1

LAG3 : Lymphocyte-activation gene 3

LILRP2 : Leukocyte immunoglobulin-like receptor pseudogene 2

NCR2 : Natural Cytotoxicity Triggering Receptor 2

NKG2A : Natural Killer Group 2 Natural Killer Group 2 member A

PD-(L)1 : Programmed death (ligand) 1

PGE2 : prostaglandin E2

S1PR1 : Sphingosine-1-phosphate receptor 1

TIGIT : T cell immunoreceptor with Ig and ITIM domains

TIM3 : T cell immunoglobulin and mucin domain-containing protein 3

Declarations

Ethics approval and consent to participate

All the patients gave an informed consent prior to inclusion. The study was conducted with the agreement of the French ethic comity (number 2012 06 12 IRB00001072) in application with the article L. 1121-1 of French law, according to the recommendations in the Helsinki declaration.

Consent for publication

Not applicable

Availability of data and materials

The datasets used and/or analyzed during the current study are available from the corresponding author on reasonable request.

Competing interests

The authors declare that they have no competing interests.

Funding

This work was supported by the “Institut National de la Sante et de la Recherche Medicale” (INSERM), Sorbonne Universite, Universite de Paris, the LabEx Immuno-Oncology, and the Institut National du Cancer (2017-PLBIO). J. Russick was supported by Sorbonne Universite.

Authors' contributions

PEJ, JR, MGB, CT, SM, NJ, CG, JG and MADD performed the experiments. MM, FP, and GB performed bioinformatic analysis. PEJ, JR, CT, MGB and IC analyzed the data. PV, LF, AL, DD and MA provided clinical samples and pathological data. IC designed and supervised the study. PE, JR, MGB and IC wrote the manuscript. AV, MCDN and LZ revised the manuscript.

Acknowledgements

We thank the Cochin hospital for contributing to the tissue collection. We also thank the CHIC (Center of Histology Imaging and Cytometry) facility of the Centre de Recherche des Cordeliers.

References

1. Vivier E, Artis D, Colonna M, Diefenbach A, Di Santo JP, Eberl G, et al. Innate Lymphoid Cells: 10 Years On. Cell. 23 2018;174(5):1054-66.

2. Schmidt L, Eskiocak B, Kohn R, Dang C, Joshi NS, DuPage M, et al. Enhanced adaptive immune responses in lung adenocarcinoma through natural killer cell stimulation. Proc Natl Acad Sci. 13 août 2019;201904253.

3. López-Soto A, Gonzalez S, Smyth MJ, Galluzzi L. Control of Metastasis by NK Cells. Cancer Cell. août 2017;32(2):135-54.

4. Morvan MG, Lanier LL. NK cells and cancer: you can teach innate cells new tricks. Nat Rev Cancer. janv 2016;16(1):7-19.

5. Villegas FR, Coca S, Villarrubia VG, Jiménez R, Chillón MJ, Jareño J, et al. Prognostic significance of tumor infiltrating natural killer cells subset CD57 in patients with squamous cell lung cancer. Lung Cancer. janv 2002;35(1):23-8.

6. Carrega P, Morandi B, Costa R, Frumento G, Forte G, Altavilla G, et al. Natural killer cells infiltrating human nonsmall-cell lung cancer are enriched in CD56 bright CD16(-) cells and display an impaired capability to kill tumor cells. Cancer. 15 févr 2008;112(4):863-75.

7. Platonova S, Cherfils-Vicini J, Damotte D, Crozet L, Vieillard V, Validire P, et al. Profound Coordinated Alterations of Intratumoral NK Cell Phenotype and Function in Lung Carcinoma. Cancer Res. 15 août 2011;71(16):5412-22.

8. Pasero C, Gravis G, Guerin M, Granjeaud S, Thomassin-Piana J, Rocchi P, et al. Inherent and Tumor-Driven Immune Tolerance in the Prostate Microenvironment Impairs Natural Killer Cell Antitumor Activity. Cancer Res. 15 avr 2016;76(8):2153-65.

9. Mamessier E, Sylvain A, Thibult M-L, Houvenaeghel G, Jacquemier J, Castellano R, et al. Human breast cancer cells enhance self tolerance by promoting evasion from NK cell antitumor immunity. J Clin Invest. 1 sept 2011;121(9):3609-22.

10. Zhang Q-F, Yin W-W, Xia Y, Yi Y-Y, He Q-F, Wang X, et al. Liver-infiltrating CD11b- CD27- NK subsets account for NK-cell dysfunction in patients with hepatocellular carcinoma and are associated with tumor progression. Cell Mol Immunol. oct 2017;14(10):819-29.

11. Rusakiewicz S, Semeraro M, Sarabi M, Desbois M, Locher C, Mendez R, et al. Immune infiltrates are prognostic factors in localized gastrointestinal stromal tumors. Cancer Res. 15 juin 2013;73(12):3499-510.

12. Cong J, Wang X, Zheng X, Wang D, Fu B, Sun R, et al. Dysfunction of Natural Killer Cells by FBP1-Induced Inhibition of Glycolysis during Lung Cancer Progression. Cell Metab. 07 2018;28(2):243-255.e5.

13. Dieu-Nosjean M-C, Antoine M, Danel C, Heudes D, Wislez M, Poulot V, et al. Long-term survival for patients with non-small-cell lung cancer with intratumoral lymphoid structures. J Clin Oncol Off J Am Soc Clin Oncol. 20 sept 2008;26(27):4410-7.

14. Goc J, Germain C, Vo-Bourgais TKD, Lupo A, Klein C, Knockaert S, et al. Dendritic Cells in Tumor-Associated Tertiary Lymphoid Structures Signal a Th1 Cytotoxic Immune Contexture and License the Positive Prognostic Value of Infiltrating CD8+ T Cells. Cancer Res. 1 févr 2014;74(3):705-15.

15. Germain C, Gnjatic S, Tamzalit F, Knockaert S, Remark R, Goc J, et al. Presence of B cells in tertiary lymphoid structures is associated with a protective immunity in patients with lung cancer. Am J Respir Crit Care Med. 1 avr 2014;189(7):832-44.

16. Catacchio I, Scattone A, Silvestris N, Mangia A. Immune Prophets of Lung Cancer: The Prognostic and Predictive Landscape of Cellular and Molecular Immune Markers. Transl Oncol. juin 2018;11(3):825-35.

17. Hervier B, Russick J, Cremer I, Vieillard V. NK Cells in the Human Lungs. Front Immunol [Internet]. 2019 [cité 5 juin 2019];10. Disponible sur: https://www.frontiersin.org/articles/10.3389/fimmu.2019.01263/full

18. Lavin Y, Kobayashi S, Leader A, Amir E-AD, Elefant N, Bigenwald C, et al. Innate Immune Landscape in Early Lung Adenocarcinoma by Paired Single-Cell Analyses. Cell. 04 2017;169(4):750-765.e17.

19. Sun H, Sun C. The Rise of NK Cell Checkpoints as Promising Therapeutic Targets in Cancer Immunotherapy. Front Immunol. 2019;10:2354.

20. Muntasell A, Ochoa MC, Cordeiro L, Berraondo P, López-Díaz de Cerio A, Cabo M, et al. Targeting NK-cell checkpoints for cancer immunotherapy. Curr Opin Immunol. avr 2017;45:73-81.

21. Neo SY, Yang Y, Record J, Ma R, Chen X, Chen Z, et al. CD73 immune checkpoint defines regulatory NK cells within the tumor microenvironment. J Clin Invest. 4 févr 2020;10.1172/JCI128895.

22. Delconte RB, Kolesnik TB, Dagley LF, Rautela J, Shi W, Putz EM, et al. CIS is a potent checkpoint in NK cell–mediated tumor immunity. Nat Immunol. juill 2016;17(7):816-24.

23. André P, Denis C, Soulas C, Bourbon-Caillet C, Lopez J, Arnoux T, et al. Anti-NKG2A mAb Is a Checkpoint Inhibitor that Promotes Anti-tumor Immunity by Unleashing Both T and NK Cells. Cell. déc 2018;175(7):1731-1743.e13.

24. Zhang Q, Bi J, Zheng X, Chen Y, Wang H, Wu W, et al. Blockade of the checkpoint receptor TIGIT prevents NK cell exhaustion and elicits potent anti-tumor immunity. Nat Immunol. 2018;19(7):723-32.

25. Chiossone L, Dumas P-Y, Vienne M, Vivier E. Natural killer cells and other innate lymphoid cells in cancer. Nat Rev Immunol. nov 2018;18(11):671-88.

26. Gillard-Bocquet M, Caer C, Cagnard N, Crozet L, Perez M, Fridman WH, et al. Lung Tumor Microenvironment Induces Specific Gene Expression Signature in Intratumoral NK Cells. Front Immunol [Internet]. 2013 [cité 29 nov 2018];4. Disponible sur: http://journal.frontiersin.org/article/10.3389/fimmu.2013.00019/abstract

27. Biton J, Ouakrim H, Dechartres A, Alifano M, Mansuet-Lupo A, Si H, et al. Impaired Tumor-Infiltrating T Cells in Patients with Chronic Obstructive Pulmonary Disease Impact Lung Cancer Response to PD-1 Blockade. Am J Respir Crit Care Med. oct 2018;198(7):928-40.

28. Bindea G, Mlecnik B, Hackl H, Charoentong P, Tosolini M, Kirilovsky A, et al. ClueGO: a Cytoscape plug-in to decipher functionally grouped gene ontology and pathway annotation networks. Bioinforma Oxf Engl. 15 avr 2009;25(8):1091-3.

29. Shannon P, Markiel A, Ozier O, Baliga NS, Wang JT, Ramage D, et al. Cytoscape: a software environment for integrated models of biomolecular interaction networks. Genome Res. nov 2003;13(11):2498-504.

30. Rowshanravan B, Halliday N, Sansom DM. CTLA-4: a moving target in immunotherapy. Blood. 8 nov 2017;blood-2017-06-741033.

31. Lavergne E, Combadiere B, Bonduelle O, Iga M, Gao J-L, Maho M, et al. Fractalkine Mediates Natural Killer-Dependent Antitumor Responses in Vivo. :8.

32. Castriconi R, Dondero A, Bellora F, Moretta L, Castellano A, Locatelli F, et al. Neuroblastoma-Derived TGF-β1 Modulates the Chemokine Receptor Repertoire of Human Resting NK Cells. J Immunol. 15 mai 2013;190(10):5321-8.

33. Yu Y-RA, Fong AM, Combadiere C, Gao J-L, Murphy PM, Patel DD. Defective antitumor responses in CX3CR1-deficient mice. Int J Cancer. 2007;121(2):316-22.

34. Stegmann KA, Robertson F, Hansi N, Gill U, Pallant C, Christophides T, et al. CXCR6 marks a novel subset of T-betloEomeshi natural killer cells residing in human liver. Sci Rep. mai 2016;6(1):26157.

35. Chiossone L, Chaix J, Fuseri N, Roth C, Vivier E, Walzer T. Maturation of mouse NK cells is a 4-stage developmental program. Blood. 28 mai 2009;113(22):5488-96.

36. Terme M, Ullrich E, Aymeric L, Meinhardt K, Coudert JD, Desbois M, et al. Cancer-Induced Immunosuppression: IL-18-Elicited Immunoablative NK Cells. Cancer Res. 1 juin 2012;72(11):2757-67.

37. Marquardt N, Kekäläinen E, Chen P, Lourda M, Wilson JN, Scharenberg M, et al. Unique transcriptional and protein-expression signature in human lung tissue-resident NK cells. Nat Commun. déc 2019;10(1):3841.

38. Stojanovic A, Fiegler N, Brunner-Weinzierl M, Cerwenka A. CTLA-4 Is Expressed by Activated Mouse NK Cells and Inhibits NK Cell IFN- Production in Response to Mature Dendritic Cells. J Immunol. 1 mai 2014;192(9):4184-91.

39. Lougaris V, Tabellini G, Baronio M, Patrizi O, Gazzurelli L, Mitsuiki N, et al. CTLA-4 regulates human Natural Killer cell effector functions. Clin Immunol. sept 2018;194:43-5.

40. Ward FJ, Dahal LN, Khanolkar RC, Shankar SP, Barker RN. Targeting the alternatively spliced soluble isoform of CTLA-4: prospects for immunotherapy? Immunotherapy. oct 2014;6(10):1073-84.

41. Walker LSK, Sansom DM. Confusing signals: Recent progress in CTLA-4 biology. Trends Immunol. 1 févr 2015;36(2):63-70.

42. Iraolagoitia XLR, Spallanzani RG, Torres NI, Araya RE, Ziblat A, Domaica CI, et al. NK Cells Restrain Spontaneous Antitumor CD8 $^{+}$ T Cell Priming through PD-1/PD-L1 Interactions with Dendritic Cells. J Immunol. 1 août 2016;197(3):953-61.

43. Böttcher JP, Bonavita E, Chakravarty P, Blees H, Cabeza-Cabrerizo M, Sammicheli S, et al. NK Cells Stimulate Recruitment of cDC1 into the Tumor Microenvironment Promoting Cancer Immune Control. Cell. févr 2018;172(5):1022-1037.e14.

44. Morandi F, Horenstein AL, Chillemi A, Quarona V, Chiesa S, Imperatori A, et al. CD56 ^{bright} CD16 $^{-}$ NK Cells Produce Adenosine through a CD38-Mediated Pathway and Act as Regulatory Cells Inhibiting Autologous CD4 $^{+}$ T Cell Proliferation. J Immunol. 1 août 2015;195(3):965-72.

45. Vivier E, Ugolini S. Regulatory Natural Killer Cells: New Players in the IL-10 Anti-Inflammatory Response. Cell Host Microbe. déc 2009;6(6):493-5.

46. Bade B, Boettcher HE, Lohrmann J, Hink-Schauer C, Bratke K, Jenne DE, et al. Differential expression of the granzymes A, K and M and perforin in human peripheral blood lymphocytes. Int Immunol. 1 nov 2005;17(11):1419-28.

47. Bratke K, Kuepper M, Bade B, Virchow JC, Luttmann W. Differential expression of human granzymes A, B, and K in natural killer cells and during CD8+ T cell differentiation in peripheral blood. Eur J Immunol. 2005;35(9):2608-16.

48. Jiang W, Chai NR, Maric D, Bielekova B. Unexpected role for granzyme K in CD56bright NK cell-mediated immunoregulation of multiple sclerosis. J Immunol Baltim Md

1950. 15 juill 2011;187(2):781-90.

49. Crome SQ, Nguyen LT, Lopez-Verges S, Yang SYC, Martin B, Yam JY, et al. A distinct innate lymphoid cell population regulates tumor-associated T cells. Nat Med. mars 2017;23(3):368-75.

50. Picard E, Godet Y, Laheurte C, Dosset M, Galaine J, Beziaud L, et al. Circulating NKp46+ Natural Killer cells have a potential regulatory property and predict distinct survival in Non-Small Cell Lung Cancer. Oncoimmunology. 2019;8(2):e1527498.

51. Topalian SL, Hodi FS, Brahmer JR, Gettinger SN, Smith DC, McDermott DF, et al. Safety, activity, and immune correlates of anti-PD-1 antibody in cancer. N Engl J Med. 28 juin 2012;366(26):2443-54.

52. Kohlhapp FJ, Broucek JR, Hughes T, Huelsmann EJ, Lusciks J, Zayas JP, et al. NK cells and CD8+ T cells cooperate to improve therapeutic responses in melanoma treated with interleukin-2 (IL-2) and CTLA-4 blockade. J Immunother Cancer. 2015;3:18.

Figure legends

Figure 1. Gene expression differential analysis of tumoral versus non-tumoral NK cells, in the discovery cohort (cohort 1)

(A) Volcano plot presenting differentially expressed genes between tumoral NK and non-tumoral NK cells. X axis displays log2 Fold changes between the two groups and Y axis the -$\log_{10}$(p.value). Differentially expressed genes (highlighted in cyan) between tumoral and non-tumoral samples were characterized by fold changes superior/inferior to 2 and with a significant p.value (<0.05). Genes of interest are colored in orange. **(B)** Heatmap of differentially expressed genes between tumoral and non-tumoral groups, organized by hierarchical clustering (after normalization of expression values). **(C)** Gene enrichment analysis for all the differentially expressed genes, using ClueGo application (Cytoscape software). **(D)** Gene enrichment analysis for down- (left panel) and up- (right panel) regulated biological processes. Color intensity of dots is proportional to the adjusted p values and size corresponds to the number of differentially expressed genes in the discovery cohort.

712 Horizontal axis represents overlap between differentially expressed genes and genes in the
713 biological processes.

714 **Figure 2. Specific gene variation between tumoral vs non-tumoral NK cells in the validation**
715 **cohort (cohort 2)**

716 NK cells were sorted from non-tumoral distant tissue (Non-Tum NK – black dots) and from
717 tumor (Tum NK – red dots) for 47 patients and total RNA were extracted and analyzed for the
718 expression of 14 genes involved in NK migration (**A**), cell activation and regulation of immune
719 responses (**B**) and cytotoxic functions (**C**) by quantitative PCR. Each dot represents a duplicate
720 measurement of the gene expression in one individual. The mean values are indicated by blue
721 dashes. Statistical differences were assessed by the Wilcoxon non-parametric-test method
722 with Graphpad software. **(D)** Heatmap of delta delta CT for tumoral and non-tumoral samples
723 of the 14 genes of interest. Hierarchical clustering identified two groups. Expression values
724 were standardized **(E)** Heatmap of fold changes of delta delta CT values between tumoral and
725 non-tumoral for the 14 genes of interest. Patient information are represented on top for each
726 sample.

727 **Figure 3. CTLA-4 protein expression in tumor infiltrating NK cells**

728 (**A, B**) Identification of CTLA-4 expressing NKp46^{+} cells in NSCLC patients by
729 immunofluorescence **(A)** or immunohistochemistry **(B)** double staining.

730 (**C, D**) CTLA-4 protein expression was analyzed in NK cells (CD3^{-} CD56^{+}), conventional T cells
731 (CD3^{+} CD56^{-} Foxp3^{-}) and regulatory T cells (CD3^{+} CD56^{-} Foxp3^{+}) by flow cytometry after
732 intracellular (Intra.) or cell surface staining of cells from tumoral (Tum) or non-tumoral (Non
733 Tum) tissue of NSCLC patients. Cells from blood were also analyzed for some patients.

734 Representative images of intracellular CTLA-4 staining are shown in (**C)** and the summary of
735 analyzes are shown in (**D)**. Statistical analyses were performed by Wilcoxon method with the
736 Graphpad software. ns: not significant.

737 **Figure 4. Intratumoral NK cells phenotype and cytokine secretion**

738 **(A)** Eomes, NKG2A, CD69, NKp44, CD107a, Fas, CXCR6, CX3CR1 and S1PR1 protein expression
739 was analyzed in NK cells ($CD3^-CD56^+$) by flow cytometry after cell surface staining of cells from
740 non-tumoral (Non-tum) or tumoral (Tum) tissue of NSCLC patients. Percentages or GeoMean
741 are presented. **(B)** Co-staining for NKp46/Eomes, NKp46/CTLA-4 and CTLA-4/NKG2A are
742 shown on $CD3^-CD56^+$ intratumoral NK cells. **(C)** Quantification of cytokines produced by NK
743 cells sorted from tumoral or non-tumoral tissue. Statistical analyses were performed by
744 Wilcoxon method with the Graphpad software. ns: not significant.

745 **Figure 5. Intratumoral NK cells reduces DC maturation**

746 (**A, B**) MHC-II and CD86 surface expression was analyzed by flow cytometry on LPS-treated
747 $CD11c^+$ DC after 2-3 days of co-culture with $CD3^-CD56^+$ intratumoral NK cells. Experimental
748 design of the co-culture experiment is shown in (**A).** (**B**) Expression of CD86 or MHC-II
749 expression on LPS-treated DC alone (DC alone) or in co-culture with $CD56^+$ cells (DC + $CD56^+$
750 cells) was analyzed. Data are represented as a ratio of mean fluorescence intensity (MFI) of
751 CD86 or MHC-II expression in DC alone (blue dots) *versus* DC + $CD56^+$ cells co-culture (red dots).
752 (**C**) The ratio of MHC-II surface protein expression on LPS-treated DC were analyzed by flow
753 cytometry after 3-4 days of culture of DC cells alone (blue dots) or in co-culture with $CD56^+$
754 cells (red dots) and in the presence of CTLA-4 blocking antibody (green triangles). Statistical
755 analyses were performed by the Wilcoxon non-parametric test with the Graph-pad software.
756 ns: not significant.

Figure 6. Correlation between CTLA-4 expression and gene signature expression in tumor vs non-tumoral NK cells

Sorted NK cells from non-tumoral distant tissue (Non-Tum NK) and tumoral (Tum NK) for 47 patients were extracted and total RNA was analyzed. CTLA-4 mRNA expression was then compared to Ct values of the 14 genes previously identified. The correlation between both values was assessed in non-tumoral and tumoral NK cells using Pearson correlation test with the Graph-pad software.

Figure 7. Clinical impact of NKp46^{+} cells in NSCLC patients

(A, B) Patients from the retrospective cohort (cohort 3) were splitted into 2 groups according to the density of intratumoral NKp46^{+} cells (**A**) or CD8^{+} cells (**B**). Separation was done by median and their overall survival was analyzed. **(C)** Patients with low density (CD8^{+} cells^{Low}) or high density (CD8^{+} cells^{High}) of CD8^{+} cells were splitted into 2 groups according to their number of intratumoral Nkp46^{+} cells and the overall survival were done in each group. Separation was done by median. (**D, E**) CD8 density of patients from the validation cohort (cohort 2) was assessed by immunohistochemistry on paraffin-embedded slides and the correlation with CTLA-4 mRNA expression in NK cells was calculated using Pearson correlation test with the Graph-pad software (**D**). (**E**) Patients from validation cohort (cohort 2) were split in 2 groups according to the density of intratumoral CD8^{+} cells (using median) and the expression of CTLA-4 mRNA was analyzed in each group. Statistical analyses were performed by the Mann-Whitney non-parametric test with the Graph-pad software.

Supplemental information

Supplemental Table S1. Discovery cohort (cohort 1).

Pathological staging and histological types of the tumors were determined according to the 2009 TNM staging system and World Health Organization. PY, packs per year; ADC, adenocarcinoma; SCC, squamous cell carcinoma.

Table S2. Top 56 up-regulated genes

Table S3. Top 56 down-regulated genes

Table S4. Validation cohort (Cohort 2)

Pathological staging and histological types of the tumors were determined according to the 2009 TNM staging system and World Health Organization. PY, packs per year; ADC, adenocarcinoma; SCC, squamous cell carcinoma

Table S5. Correlation between intra-tumoral NK cells and B, mature DC or $CD8^+$ T cell density

Coefficients of correlation of NK cell density with B, mature DC or $CD8^+$ T cells density. Spearman correlations (*r^2) were calculated with the Kendal method using R studio software.

Fig S1. Association between clinical parameters and groups 1 and 2 defined by unsupervised clustering.

Bar plot representing the repartition of patients among assigned groups defined in figure 2E. Colors indicate the different categories for each clinical parameter.

Fig.S2. Multicolor immunofluorescence of formalin-fixed paraffin-embedded tumoral tissues from patients with melanoma. breast or renal cancer.

The double-staining of NKp46 (Red) and CTLA-4 (White) was performed in intra-tumoral tissues of several cancer types. Nucleus was stained with Dapi (Blue).

Fig.S3. Association between clinical parameters and CTLA-4 expression by intratumoral NK cells and clinical impact of CTLA-4 expressing NK cells.

(A) Bar plot representing the repartition of patients with high and low CTLA-4 expressing NK. Colors indicate the different categories for each clinical parameter. **(B)** Overall survival between patients with high and low CTLA-4 expressing NK cells.

Fig S4. Reduced cytotoxicity in redirected lysis assay

Cytoxocity against K562 or P815 mastocytoma was determined by degranulation assay, using CD107a labeling and FACS analysis. IL-2-stimulated PBMC from blood of NSCLC patients, or IL-2-stimulated tumor infiltrating lymphocytes (TIL) were used as effector cells, at a ratio E:T of 10:1, in the presence or not of anti-CD16 mAb for redirected lysis against P815 cells. The percentages indicated give the proportion of CD107 positive PBMC after gating on $CD3^-$ $CD56^+$ NK cells.

Fig. S5. Gating strategy

FACS analysis was done by selecting the live cells by morphology (FSC/SSC), removal of doublets (FSC-A/FSC-H and SSC-A/SSC-H) and live cells (Live/Dead- cells). NK cells were then characterized as $CD3^-CD56^+$ among the $CD45^+$ cells and DC cells as $CD11c^+$, among the CD45+ cells.

Fig.S6. Example of NKp46 staining by IHC in the retrospective cohort (cohort 3).

Fig.S7. Clinical impact of $NKp46^+$ cell density according to the stage, the tumor size or the histology of the tumors, in the retrospective cohort (cohort 3).

(A - D) Patients from the retrospective cohort (cohort 3) were splitted into 2 groups according to density of intra-tumoral NKp46^{+} cells. Separation was done by median and their overall survival was analyzed according to (A) the stage (stage I and II), (B) the size, (C) the histology (ADC = adenocarcinoma, SCC = squamous cell carcinoma) of the tumor, or (D) the Chronic Obstructive Pulmonary Disease (COPD) status of the patient.

Fig.S8. Clinical impact of NKp46^{+} cells according to B or dendritic cells infiltration in the retrospective cohort (cohort 3).

Patients with low density or high density of B cells (B cells ^{Low} and B cells ^{High}, respectively – separated by median, and determined as surface of CD20 B-cell follicles in square millimeter per tumor surface) or with low density or high density of mature DC-LAMP expressing dendritic cells (DC cells ^{Low} and DC cells ^{High}, respectively – separated by median, and determined as the numbers of DC-LAMP^{+} cells per tumor surface) were splitted into 2 groups according to their number of intra-tumoral Nkp46^{+} cells and the overall survival were analyzed in each group.

Fig S9. Correlation between CTLA-4 and T cells in NSCLC

(A) Correlation between the percentages of CTLA-4^{+} NK cells and the percentage of CD3^{+} T cells in the tumor was analyzed, based on flow cytometry data. The pearson coefficient of correlation and the p-value are represented. **(B)** The correlation between *CTLA4* and *CD4* or between *CTLA4* and *CD8* gene expression, measured as transcripts per million (TPM), was analyzed in lung adenocarcinoma (LUAD), and lung squamous cell carcinoma (LUSC), with gene expression profiling interactive analysis (GEPIA2) tool (http://gepia2.cancer.pku.cn/), in TCGA database. The pearson coefficient of correlation between *CTLA4* and *CD4* or *CD8* expression and the p-value are represented for each tumor type.

Supplemental table 1: Clinical characteristics of NSCLC patients of the discovery cohort

Patient	Age	Sex	Tobacco (PY)	Histology	Stage (2009)
P1	61	M	45	ADC	IB
P2	62	F	50	ADC	IB
P3	59	F	>10	ADC	IB
P4	72	F	60	ADC	IB
P5	78	F	50	ADC	IB
P6	60	M	50	ADC	IIA
P7	61	M	50	ADC	IIIA
P8	71	F	40	SCC	IB
P9	57	M	80	SCC	IB
P10	79	M	50	SCC	IIB
P11	80	M	40	SCC	IIB
P12	84	M	>10	SCC	IIIA

Pathological staging and histological types of the tumors were determined according to the 2009 TNM staging system and World Health Organization. PY: packs per year. ADC: Adenocarcinoma; SCC: Squamous Cell Carcinoma.

Supplemental table 2: List of the genes that are over-expressed (more than 4-fold change) in intra-tumoral compared to non-tumoral NK cells

Gene name	Log2 FC expression (T vs NT)	adj p-value
CXCL13	5.01	9.8e-04
EPCAM	4.26	4.9e -04
SOST	4.21	9.8e -04
NCR2	4.17	1.5e -03
SPP1	3.97	4.9e-04
FNDC4	3.77	4.9e-03
SIX4	3.72	2.4e-03
LILRP2	3.63	1.5e-03
PLS3	3.59	4.9e-03
APOD	3.53	2.1e-02
FCRL4	3.40	9.8e-04
P4HA2	3.32	4.9e-04
XAGE1A	3.29	9.3e-03
PHOSPHO2-KLHL23	3.25	4.9e-04
GEM	3.21	4.9e-04
CHRNA5	3.20	4.9e-04
ITGA1	3.16	1.5e-03
TM4SF1	3.13	4.9e-04
CNN3	3.09	9.8e-04
CHRNA3	3.09	4.9e-04

KRT6C	2.93	9.3e-03
CEACAM5	2.89	9.3e-03
CDH17	2.82	2.1e-02
IGLL5	2.81	4.9e-03
PRRG4	2.81	9.8e-04
SFTA3	2.78	1.2e-02
CEACAM6	2.73	1.2e-02
CAMK4	2.72	9.8e-04
TRAT1	2.67	4.9e-04
ELF3	2.64	1.2e-02
KRT6A	2.60	4.2e-02
CYR61	2.59	2.4e-03
AGR2	2.57	3.4e-03
ITM2C	2.56	4.9e-03
NDFIP2	2.54	1.6e-02
IRX3	2.53	4.2e-02
SCNN1A	2.50	2.7e-02
CTLA4	2.50	4.9e-04
CRYAB	2.50	9.8e-04
KIAA1644	2.49	4.9e-04
BAG3	2.48	4.9e-04
LAPTM4B	2.48	4.9e-04
CLDN1	2.47	3.4e-03
KRT18P55	2.47	4.9e-04

SERPINH1	2.47	3.4e-03
SLC6A14	2.46	1.2e-02
CEACAM3	2.45	2.1e-02
TMPRSS3	2.44	4.9e-03
PLOD2	2.40	9.8e-04
ANLN	2.38	2.1e-02
PIK3R6	2.35	2.4e-03
TPSAB1	2.34	4.2e-02
GSG2	2.34	2.4e-03
SERPINE1	2.34	2.4e-03
TMEM200A	2.33	6.8e-03

852

853

Supplemental table 3: List of the genes that are under-expressed (more than 4-fold change) in intra-tumoral compared to non-tumoral NK cells

Gene name	Log2 FC expression (T vs NT)	adj p-val
FABP4	-4.03	4.9e-04
PPARG	-3.05	4.9e-04
SCGB1A1	-2.88	4.9e-04
CX3CR1	-2.66	4.9e-04
AKR1CL1	-2.54	4.9e-04
PLEKHG3	-2.35	4.9e-04
TTLL11	-2.05	4.9e-04
RGS9	-2.05	4.9e-04
GPR141	-1.95	4.9e-04
GLDN	-4.10	9.8e-04
STAC	-3.39	9.8e-04
MARCO	-3.09	9.8e-04
PHYHD1	-2.49	9.8e-04
PLBD1	-2.31	9.8e-04
VSIG4	-2.24	9.8e-04
MSR1	-2.12	9.8e-04
ZNF69	-2.11	9.8e-04
LRP1	-1.95	9.8e-04
TM7SF4	-2.83	1.5e-03
PODN	-3.16	2.4e-03

LIPC	-2.77	2.4e-03
B3GAT1	-2.05	2.4e-03
LPL	-3.64	3.4e-03
KRT72	-2.73	3.4e-03
SPIRE2	-2.57	3.4e-03
HBB	-2.21	3.4e-03
NEIL1	-2.17	3.4e-03
PLXDC2	-2.08	3.4e-03
AOC3	-2.34	3.9e-03
CD6	-2.52	4.9e-03
COLEC12	-2.39	4.9e-03
CPVL	-1.96	6.8e-03
CLEC9A	-3.07	9.3e-03
SERPINB2	-2.88	9.3e-03
RBP4	-2.40	9.3e-03
FEZ1	-2.02	9.3e-03
ADCY9	-2.48	1.2e-02
S100A12	-2.23	1.2e-02
SFTPC	-2.19	1.2e-02
C1QA	-2.03	1.2e-02
MT1G	-4.22	1.6e-02
CYP27A1	-2.67	1.6e-02
NCF2	-2.41	1.6e-02
ASMT	-2.24	1.6e-02

MT1H	-1.99	1.6e-02
MT1M	-2.69	2.1e-02
SIGLEC1	-2.26	2.1e-02
PRSS23	-2.00	2.1e-02
TLR8	-1.94	2.7e-02
APOC1	-2.79	3.4e-02
PDZD4	-2.00	3.4e-02
P2RY13	-2.17	4.2e-02
AKR1E2	-2.05	4.2e-02

856

857

858 **Supplemental table 4: Clinical characteristics of NSCLC patients of the validation cohort**

Patients	Gender	Age	Tobacco (PY)	Histological Type	TNM	Stade
P1	M	71	30	LCNEC	pT2aN2Mx	IIIA
P2	F	68	30	SCC	pT2bN0	IIA
P3	M	63	80	SCC	pT3N1Mx	IIIA
P4	F	64	20	ADC	pT2aN2	IIIA
P5	F	68	0	ADC	pT1bN0	IA
P6	F	62	N/A	ADC	pT1bN0	IA
P7	M	79	50	SCC	pT2aN0	IB
P8	F	76	40	ADC	pT2aN0Mx	IB
P9	F	57	30	SCC	ypT2aN0	IB
P10	F	70	50	SCC	pT2aN0	IB
P11	F	61	15	ADC	pT2aN1Mx	IIB
P12	F	80	0	ADC	pT2aN2Mx	IIIA
P13	F	75	25	ADC	pT3N0	IIB
P14	F	65	80	SCC	pT2aN0	IB
P15	M	78	N/A	LCNEC	pT3N0Mx	IIB
P16	F	73	50	SCC	pT2aN0	IB
P17	M	78	45	SCC	pT2aN1	IIB
P18	F	51	28	ADC	pT2aN0	IB
P19	M	66	50	SCC	pT2aN0	IB
P20	M	72	17	SCC	pT2bN1	IIB
P21	M	77	60	ADC	pT2aPL2N0	IB

P22	M	67	80	SCC	pT1bN0	IA
P23	F	58	30	ADC	pT2aN0	IB
P24	F	59	20	ADC	pT2aN0	IB
P25	M	66	50	ADC	pT2aPL1N0Mx	IB
P26	M	45	30	SCC	pT3N1Mx	IIIA
P27	M	63	50	ADC	pT1aN0	IA
P28	M	65	50	SCC	pT2aN0	IB
P29	F	30	N/A	ADC	pT2aPL2N2	IIIA
P30	F	84	0	ADC	pT2b(PL3)N0	IIA
P31	M	73	30	SCC	pT3N1Mx	IIA
P32	F	58	20	SCC	pT3N2	IIIA
P33	M	62	40	ADC-LCNEC	pT1aN1	IIA
P34	F	84	0	ADC	pT2aN0	IB
P35	M	82	20	SCC	pT2aN0Mx	IB
P36	F	76	18	ADC	pT2b(PL2)N1	IIB
P37	F	57	25	ADC	pT2aN0Mx	IB
P38	M	63	50	SCC	pT3N1	IIIA
P39	M	63	N/A	ADC	pT2aN0	IB
P40	F	57	10	ADC	pT2aN0	IB
P41	F	N/A	N/A	ADC	pT2bN1	IIB
P42	F	69	0	ADC	pT2aN0	IB
P43	M	57	37	SCC	pT2bN1	IIB
P44	M	71	75	SCC	pT3N0Mx	IIB
P45	M	69	50	SCC	pT2bN0Mx	IB

P46	F	76	50	SCC	pT2bNx	IIA
P47	F	80	N/A	SCC	pT3N0Mx	IIB

SCC squamous cell carcinoma, ADC adenocarcinoma, LCNEC large cell neuroendocrine carcinoma

Supplemental table 5: Correlation between intra-tumoral NK cells and B, mature DC or $CD8^+$ T cell density

	NK cells	B cells	Mature DC	$CD8^+$ T cells
NK cells	1*	0.08*	0.15*	0.025*

***spearman correlation coefficient**

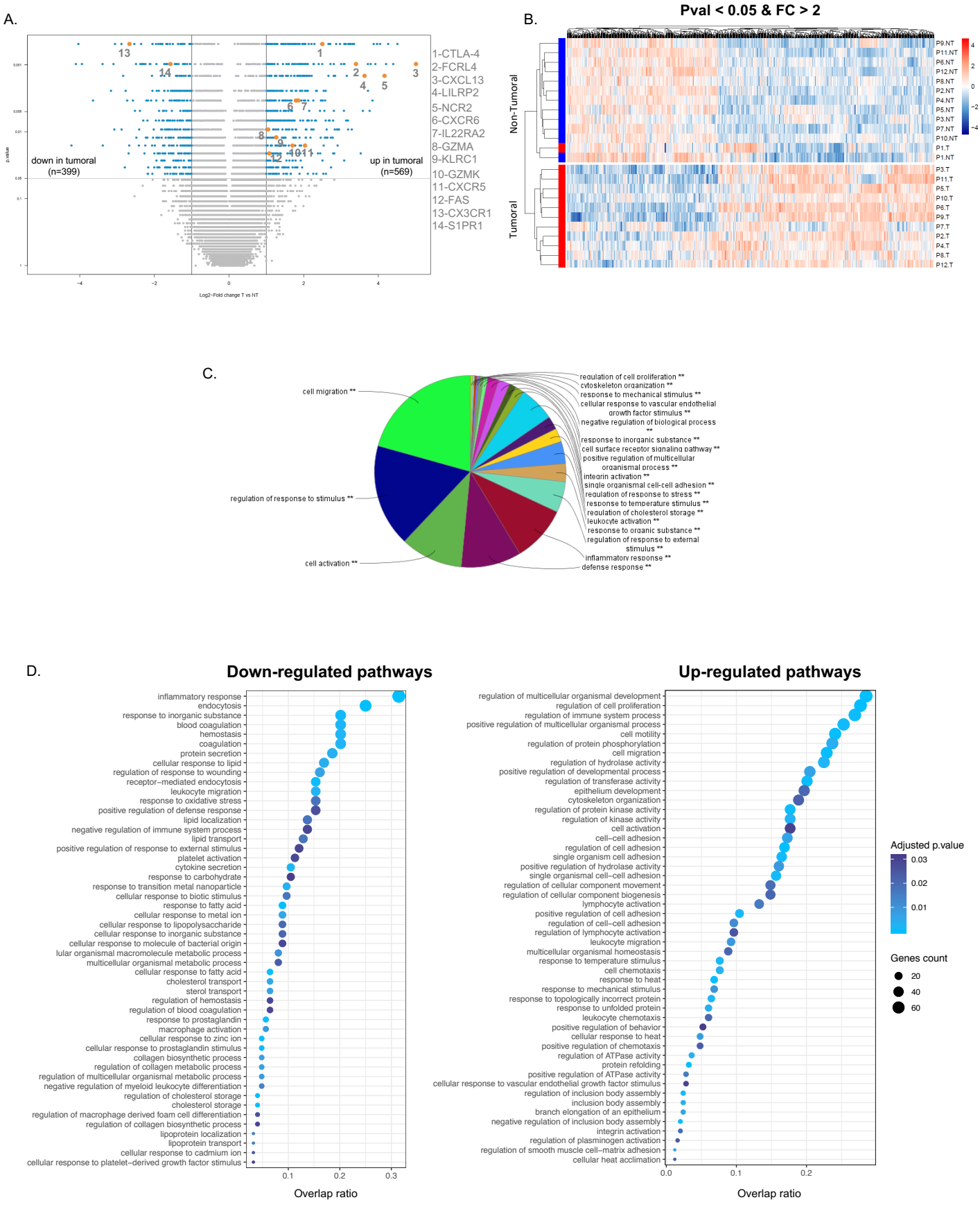
A.
B.
Pval < 0.05 & FC > 2
C.
D.
Down-regulated pathways
Up-regulated pathways
down in tumoral (n=399)
up in tumoral (n=569)
1-CTLA-4
2-FCRL4
3-CXCL13
4-LILRP2
5-NCR2
6-CXCR6
7-IL22RA2
8-GZMA
9-KLRC1
10-GZMK
11-CXCR5
12-FAS
13-CX3CR1
14-S1PR1
Non-Tumoral
Tumoral
cell migration **
regulation of response to stimulus **
cell activation **
regulation of cell proliferation **
cytoskeleton organization **
response to mechanical stimulus **
cellular response to vascular endothelial growth factor stimulus **
negative regulation of biological process **
response to inorganic substance **
cell surface receptor signaling pathway **
positive regulation of multicellular organismal process **
integrin activation **
single organismal cell-cell adhesion **
regulation of response to stress **
response to temperature stimulus **
regulation of cholesterol storage **
leukocyte activation **
response to organic substance **
regulation of response to external stimulus **
inflammatory response **
defense response **
Overlap ratio
Adjusted p.value
Genes count

Fig. 1

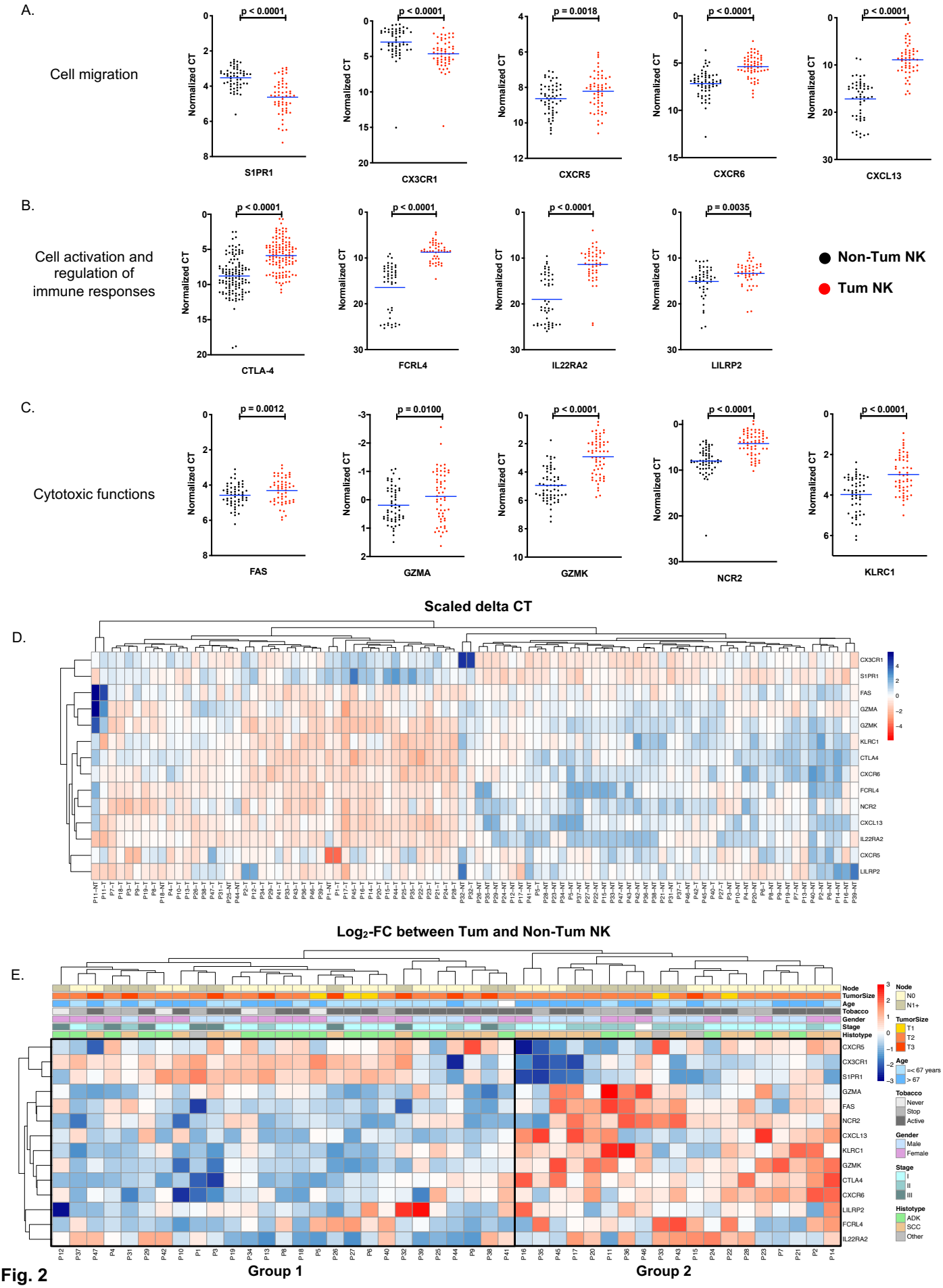
A.
Cell migration
p < 0.0001
p < 0.0001
p = 0.0018
p < 0.0001
p < 0.0001
Normalized CT
S1PR1
CX3CR1
CXCR5
CXCR6
CXCL13
B.
Cell activation and regulation of immune responses
p < 0.0001
p < 0.0001
p < 0.0001
p = 0.0035
CTLA-4
FCRL4
IL22RA2
LILRP2
Non-Tum NK
Tum NK
C.
Cytotoxic functions
p = 0.0012
p = 0.0100
p < 0.0001
p < 0.0001
p < 0.0001
FAS
GZMA
GZMK
NCR2
KLRC1
D.
Scaled delta CT
CX3CR1
S1PR1
FAS
GZMA
GZMK
KLRC1
CTLA4
CXCR6
FCRL4
NCR2
CXCL13
IL22RA2
CXCR5
LILRP2
E.
Log2-FC between Tum and Non-Tum NK
Node
TumorSize
Age
Tobacco
Gender
Stage
Histotype
CXCR5
CX3CR1
S1PR1
GZMA
FAS
NCR2
CXCL13
KLRC1
GZMK
CTLA4
CXCR6
LILRP2
FCRL4
IL22RA2
N0
N1+
T1
T2
T3
=< 67 years
> 67
Never
Stop
Active
Male
Female
I
II
III
ADK
SCC
Other
Group 1
Group 2

Fig. 2

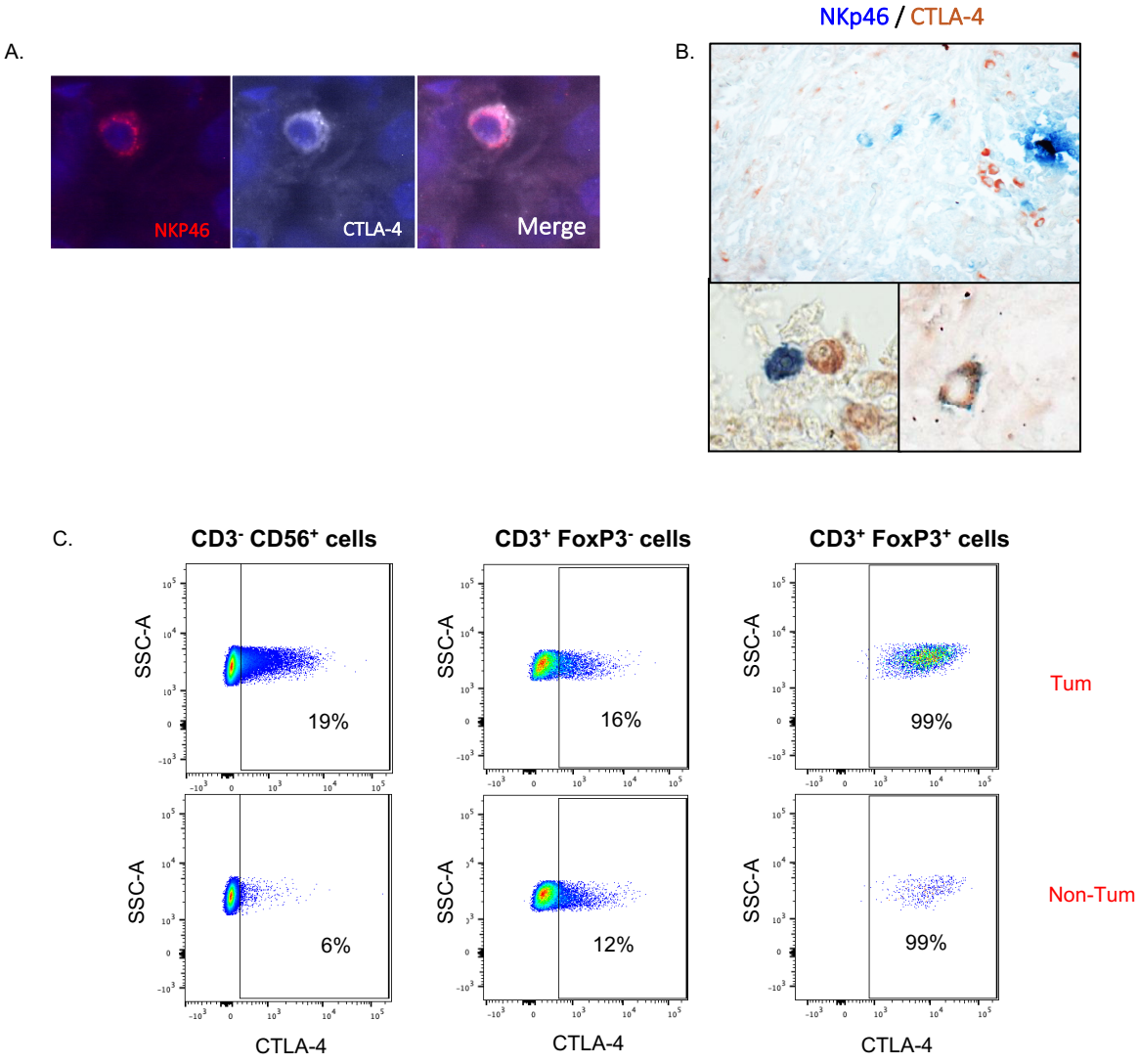
A.
NKP46
CTLA-4
Merge
B.
NKp46 / CTLA-4
C.
CD3⁻ CD56⁺ cells
CD3⁺ FoxP3⁻ cells
CD3⁺ FoxP3⁺ cells
SSC-A
CTLA-4
19%
16%
99%
6%
12%
99%
Tum
Non-Tum
D.
NK cells
Tconv
Treg
% of CTLA-4⁺ cells
p=0.016
p=0.044
p=0.016
ns
Non-Tum
Tum
Blood
Intracellular
Cell surface

Fig. 3

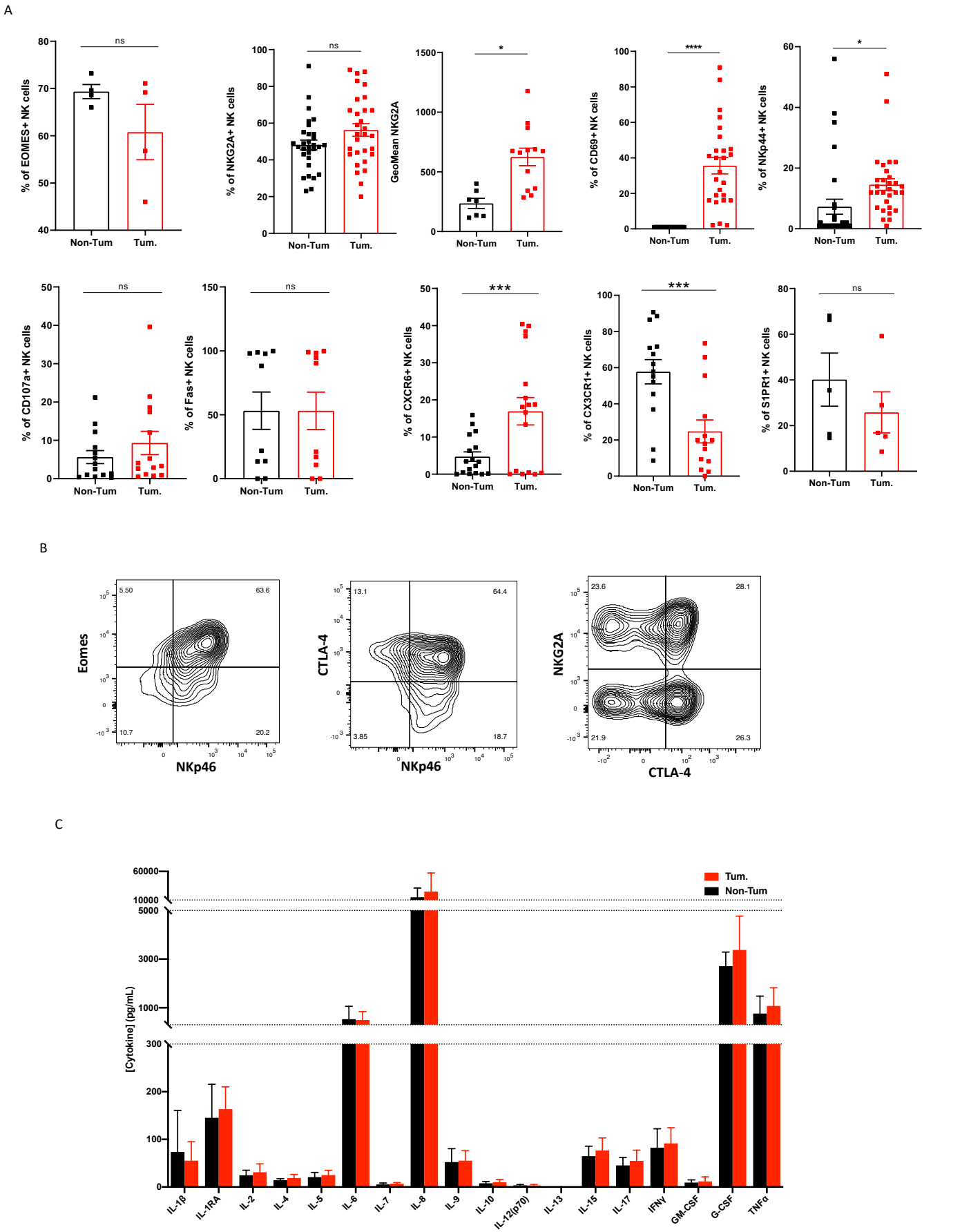
A
% of EOMES+ NK cells
% of NKG2A+ NK cells
GeoMean NKG2A
% of CD69+ NK cells
% of NKp44+ NK cells
% of CD107a+ NK cells
% of Fas+ NK cells
% of CXCR6+ NK cells
% of CX3CR1+ NK cells
% of S1PR1+ NK cells
ns
*
****
***
Non-Tum
Tum.
B
Eomes
NKp46
CTLA-4
NKG2A
5.50
63.6
10.7
20.2
13.1
64.4
3.85
18.7
23.6
28.1
21.9
26.3
C
[Cytokine] (pg/mL)
Tum.
Non-Tum
IL-1β
IL-1RA
IL-2
IL-4
IL-5
IL-6
IL-7
IL-8
IL-9
IL-10
IL-12(p70)
IL-13
IL-15
IL-17
IFNγ
GM-CSF
G-CSF
TNFα

Fig. 4

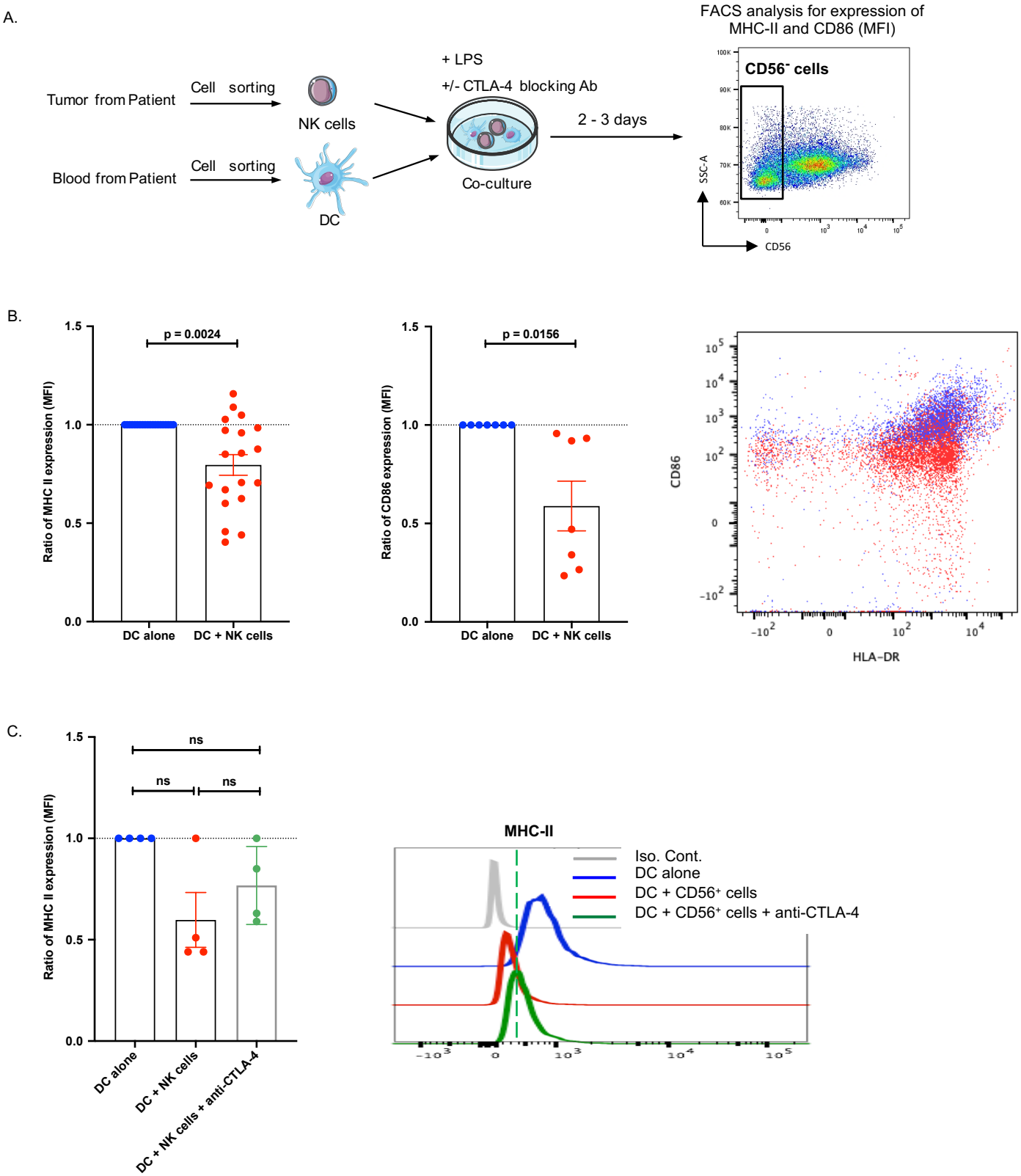
A.
Tumor from Patient
Cell sorting
NK cells
Blood from Patient
Cell sorting
DC
+ LPS
+/- CTLA-4 blocking Ab
Co-culture
2 - 3 days
FACS analysis for expression of MHC-II and CD86 (MFI)
CD56- cells
SSC-A
CD56
B.
Ratio of MHC II expression (MFI)
p = 0.0024
DC alone
DC + NK cells
Ratio of CD86 expression (MFI)
p = 0.0156
DC alone
DC + NK cells
CD86
HLA-DR
C.
Ratio of MHC II expression (MFI)
ns
ns
ns
DC alone
DC + NK cells
DC + NK cells + anti-CTLA-4
MHC-II
Iso. Cont.
DC alone
DC + CD56+ cells
DC + CD56+ cells + anti-CTLA-4

Fig. 5

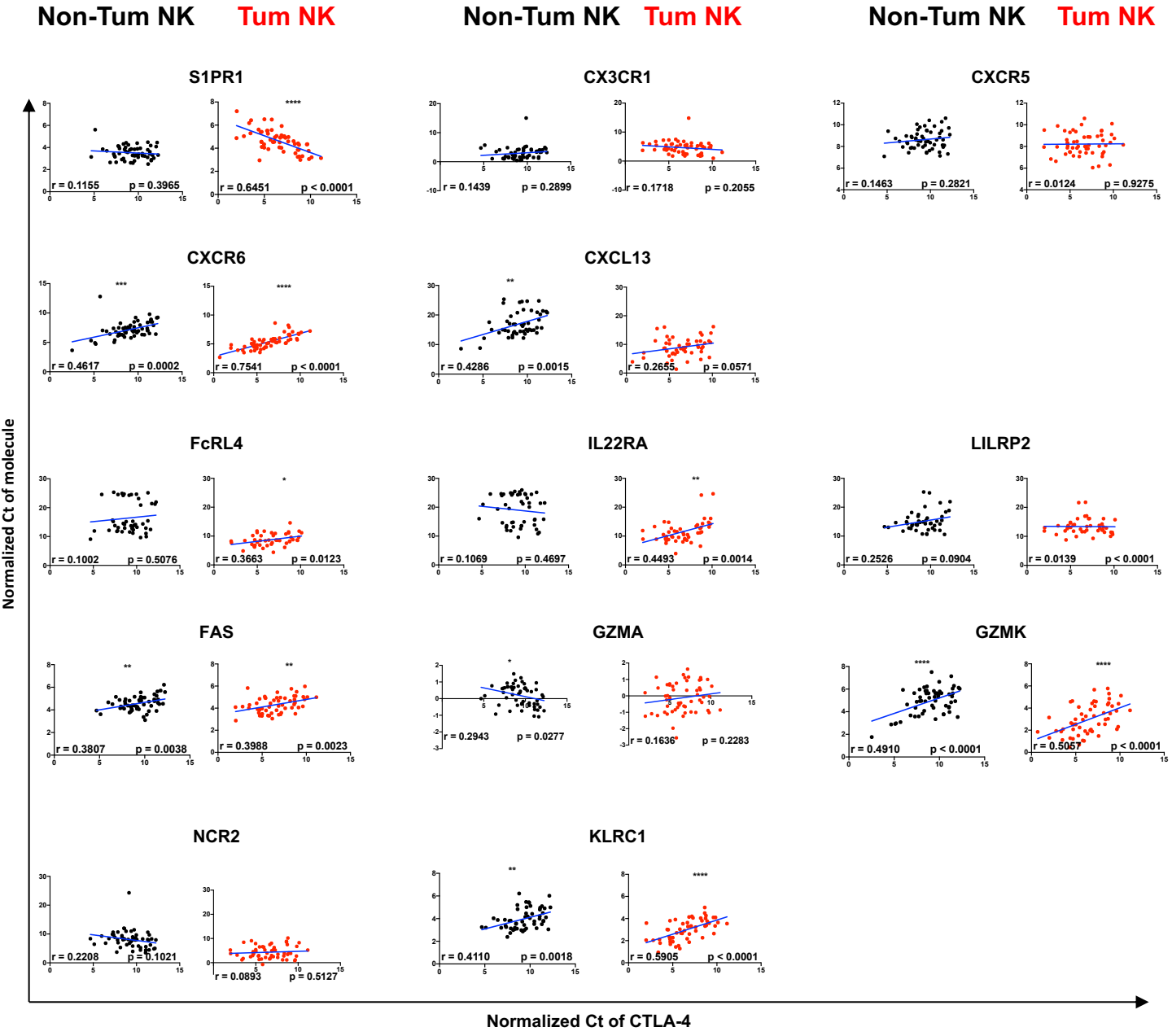
Non-Tum NK
Tum NK
Non-Tum NK
Tum NK
Non-Tum NK
Tum NK
S1PR1
r = 0.1155 p = 0.3965
r = 0.6451 p < 0.0001
CX3CR1
r = 0.1439 p = 0.2899
r = 0.1718 p = 0.2055
CXCR5
r = 0.1463 p = 0.2821
r = 0.0124 p = 0.9275
CXCR6
r = 0.4617 p = 0.0002
r = 0.7541 p < 0.0001
CXCL13
r = 0.4286 p = 0.0015
r = 0.2655 p = 0.0571
FcRL4
r = 0.1002 p = 0.5076
r = 0.3663 p = 0.0123
IL22RA
r = 0.1069 p = 0.4697
r = 0.4493 p = 0.0014
LILRP2
r = 0.2526 p = 0.0904
r = 0.0139 p < 0.0001
FAS
r = 0.3807 p = 0.0038
r = 0.3988 p = 0.0023
GZMA
r = 0.2943 p = 0.0277
r = 0.1636 p = 0.2283
GZMK
r = 0.4910 p < 0.0001
r = 0.5057 p < 0.0001
NCR2
r = 0.2208 p = 0.1021
r = 0.0893 p = 0.5127
KLRC1
r = 0.4110 p = 0.0018
r = 0.5905 p < 0.0001
Normalized Ct of molecule
Normalized Ct of CTLA-4

Fig. 6

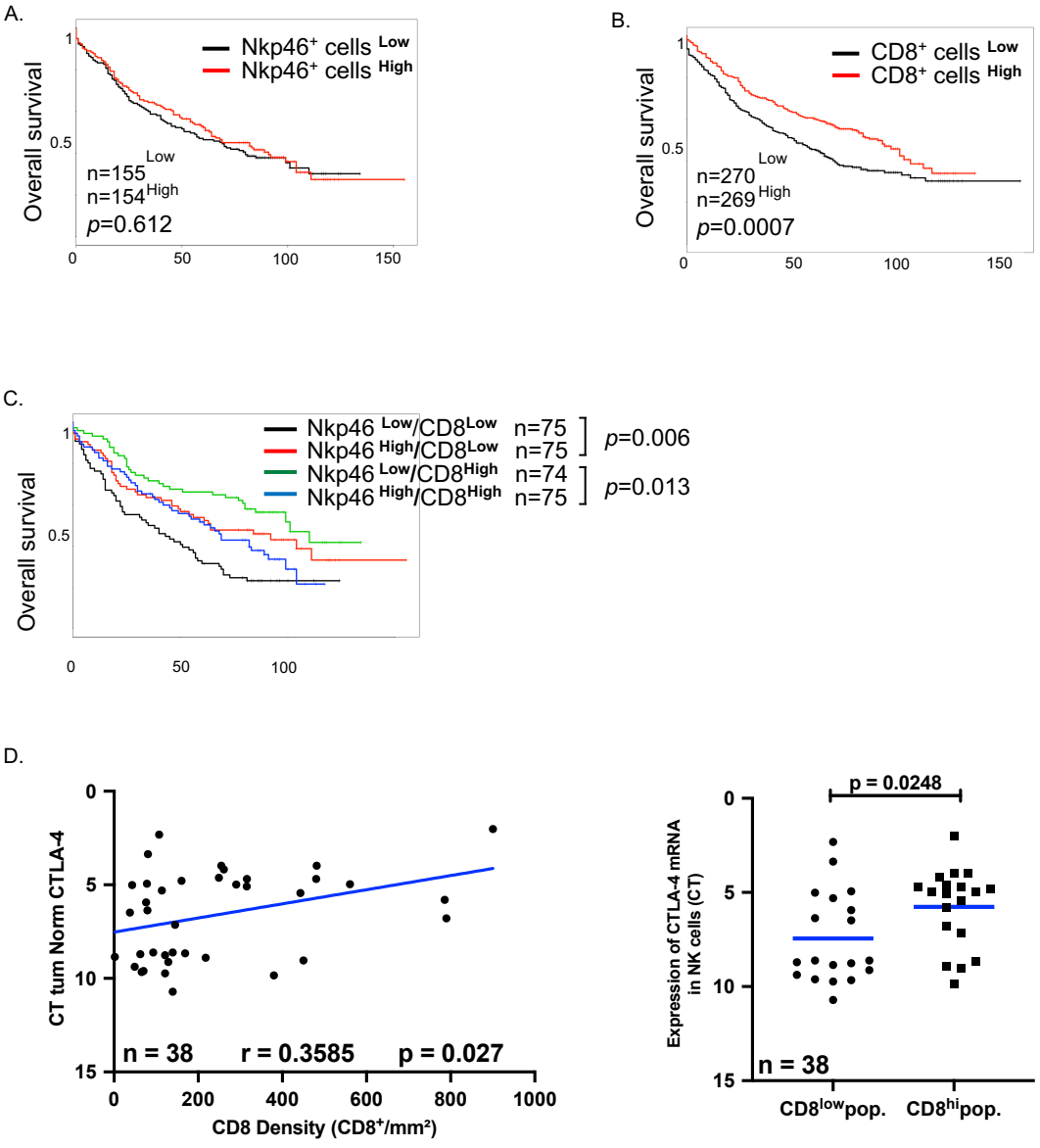
A.
Nkp46+ cells Low
Nkp46+ cells High
Overall survival
n=155 Low
n=154 High
p=0.612
B.
CD8+ cells Low
CD8+ cells High
Overall survival
n=270 Low
n=269 High
p=0.0007
C.
Nkp46 Low/CD8Low n=75
Nkp46 High/CD8Low n=75
Nkp46 Low/CD8High n=74
Nkp46 High/CD8High n=75
p=0.006
p=0.013
Overall survival
D.
CT tum Norm CTLA-4
n = 38 r = 0.3585 p = 0.027
CD8 Density (CD8+/mm²)
p = 0.0248
Expression of CTLA-4 mRNA in NK cells (CT)
n = 38
CD8low pop.
CD8hi pop.

Fig. 7

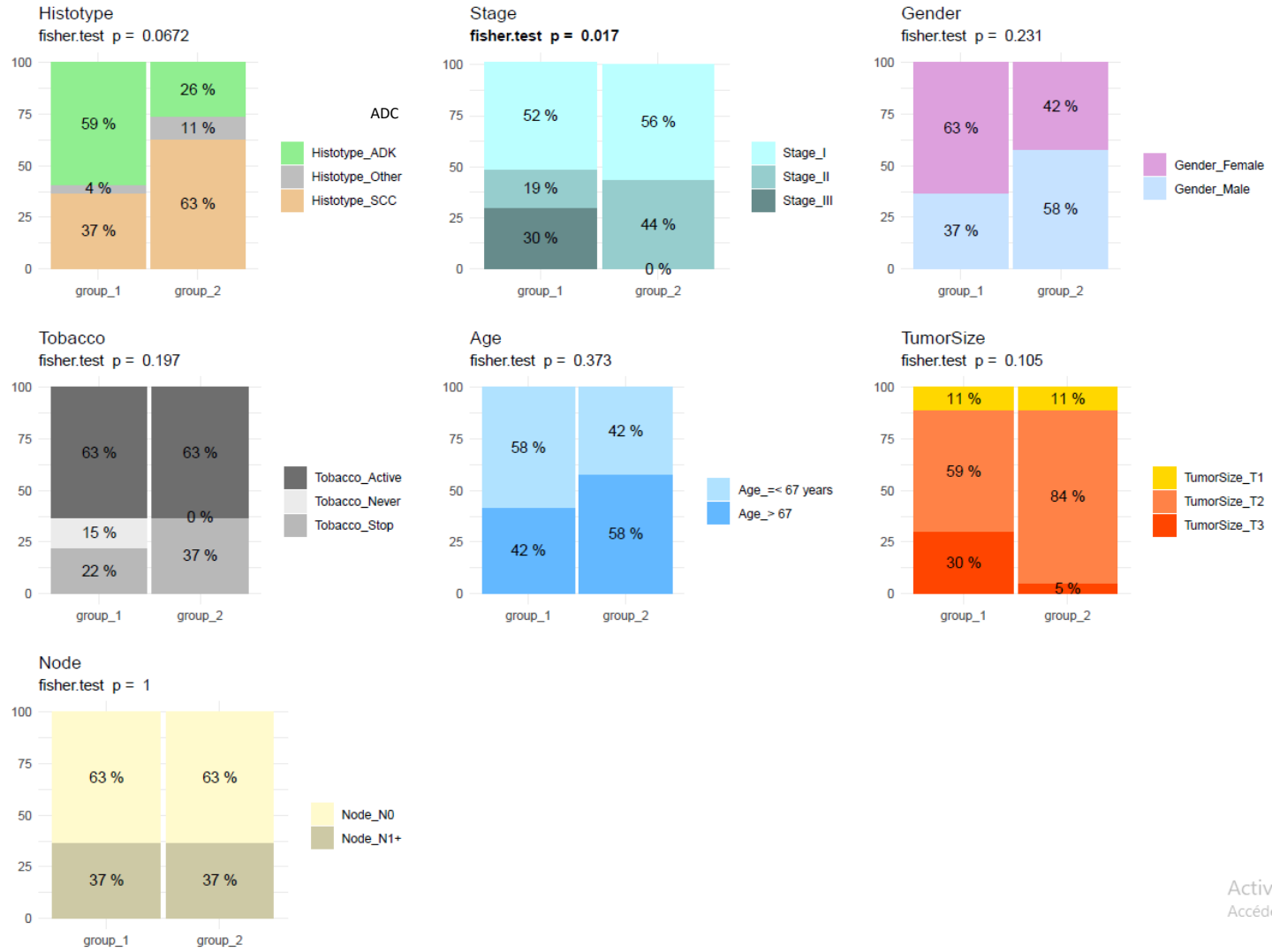
Histotype
fisher.test p = 0.0672
59 %
4 %
37 %
26 %
11 %
63 %
ADC
Histotype_ADK
Histotype_Other
Histotype_SCC
Stage
fisher.test p = 0.017
52 %
19 %
30 %
56 %
44 %
0 %
Stage_I
Stage_II
Stage_III
Gender
fisher.test p = 0.231
63 %
37 %
42 %
58 %
Gender_Female
Gender_Male
Tobacco
fisher.test p = 0.197
63 %
15 %
22 %
63 %
0 %
37 %
Tobacco_Active
Tobacco_Never
Tobacco_Stop
Age
fisher.test p = 0.373
58 %
42 %
42 %
58 %
Age_=< 67 years
Age_> 67
TumorSize
fisher.test p = 0.105
11 %
59 %
30 %
11 %
84 %
5 %
TumorSize_T1
TumorSize_T2
TumorSize_T3
Node
fisher.test p = 1
63 %
37 %
63 %
37 %
Node_N0
Node_N1+
100
75
50
25
0
group_1
group_2

Fig.S1

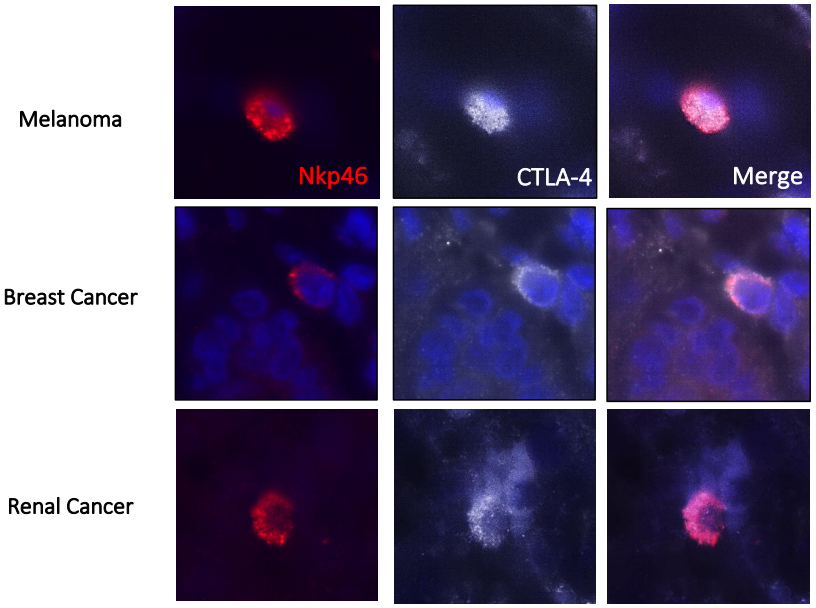

Fig.S2

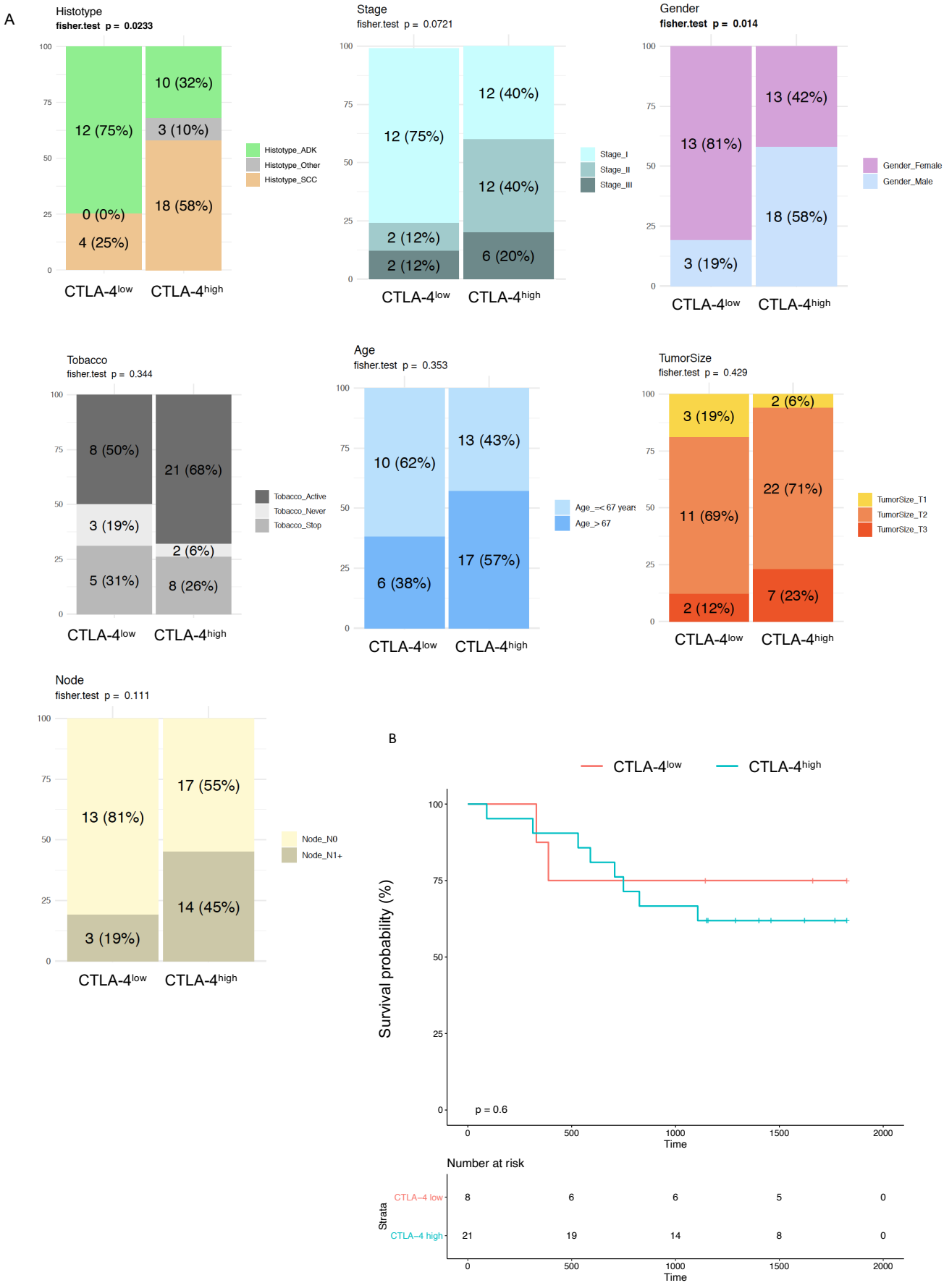
A
Histotype
fisher.test p = 0.0233
12 (75%)
0 (0%)
4 (25%)
10 (32%)
3 (10%)
18 (58%)
Histotype_ADK
Histotype_Other
Histotype_SCC
Stage
fisher.test p = 0.0721
12 (75%)
2 (12%)
2 (12%)
12 (40%)
12 (40%)
6 (20%)
Stage_I
Stage_II
Stage_III
Gender
fisher.test p = 0.014
13 (81%)
3 (19%)
13 (42%)
18 (58%)
Gender_Female
Gender_Male
Tobacco
fisher.test p = 0.344
8 (50%)
3 (19%)
5 (31%)
21 (68%)
2 (6%)
8 (26%)
Tobacco_Active
Tobacco_Never
Tobacco_Stop
Age
fisher.test p = 0.353
10 (62%)
6 (38%)
13 (43%)
17 (57%)
Age_=< 67 years
Age_> 67
TumorSize
fisher.test p = 0.429
3 (19%)
11 (69%)
2 (12%)
2 (6%)
22 (71%)
7 (23%)
TumorSize_T1
TumorSize_T2
TumorSize_T3
Node
fisher.test p = 0.111
13 (81%)
3 (19%)
17 (55%)
14 (45%)
Node_N0
Node_N1+
CTLA-4low
CTLA-4high
B
Survival probability (%)
p = 0.6
Time
Number at risk
Strata
CTLA-4 low
CTLA-4 high
8
6
6
5
0
21
19
14
8
0

Fig.S3

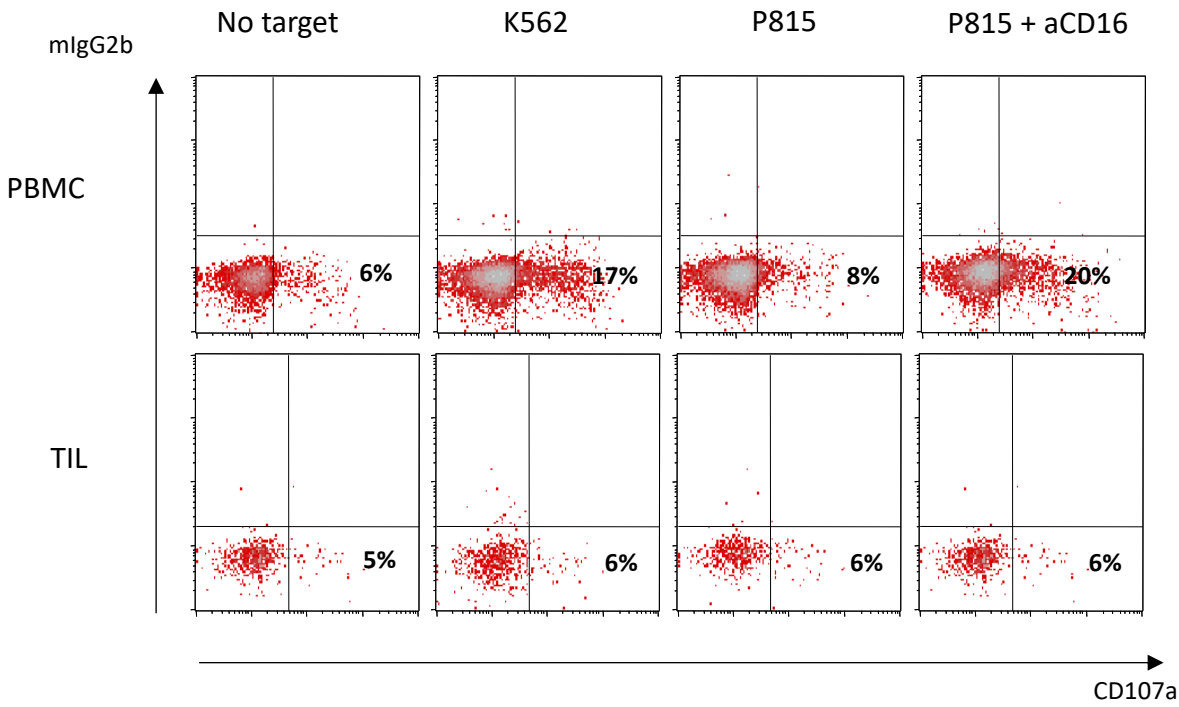
No target
K562
P815
P815 + aCD16
mIgG2b
PBMC
TIL
6%
17%
8%
20%
5%
6%
6%
6%
CD107a

Fig.S4

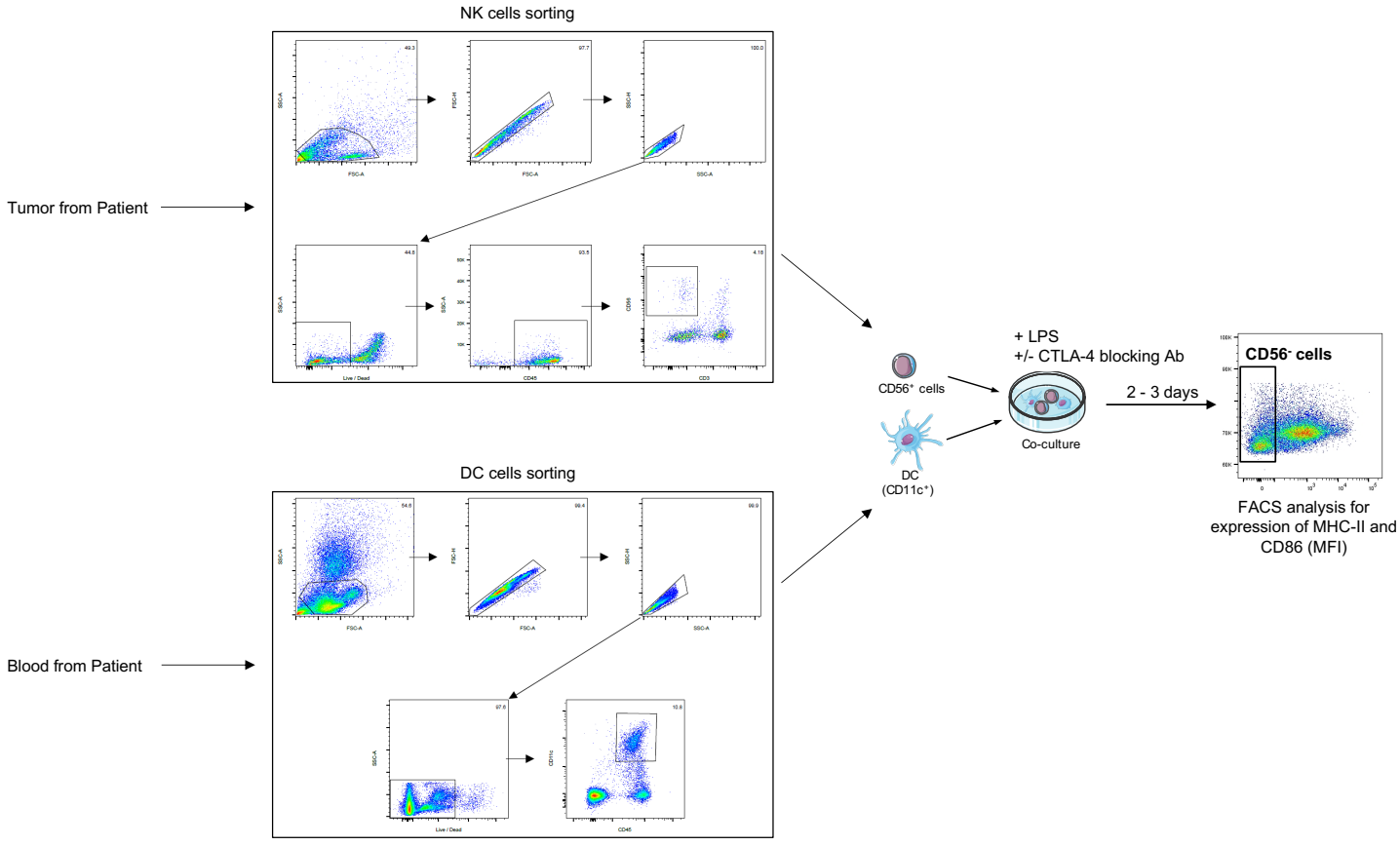
NK cells sorting
Tumor from Patient
Live / Dead
CD45
CD3
DC cells sorting
Blood from Patient
CD11c
CD56+ cells
DC
(CD11c+)
+ LPS
+/- CTLA-4 blocking Ab
Co-culture
2 - 3 days
CD56- cells
FACS analysis for
expression of MHC-II and
CD86 (MFI)

Fig.S5

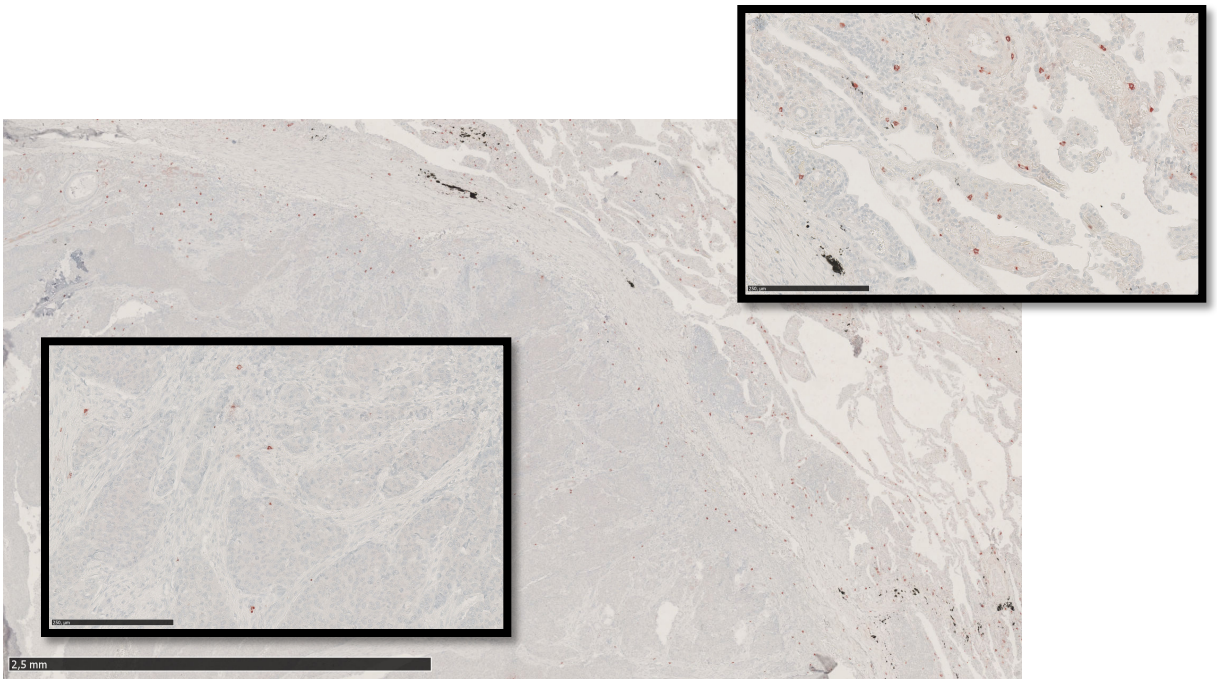

Nkp46 staining

Fig.S6

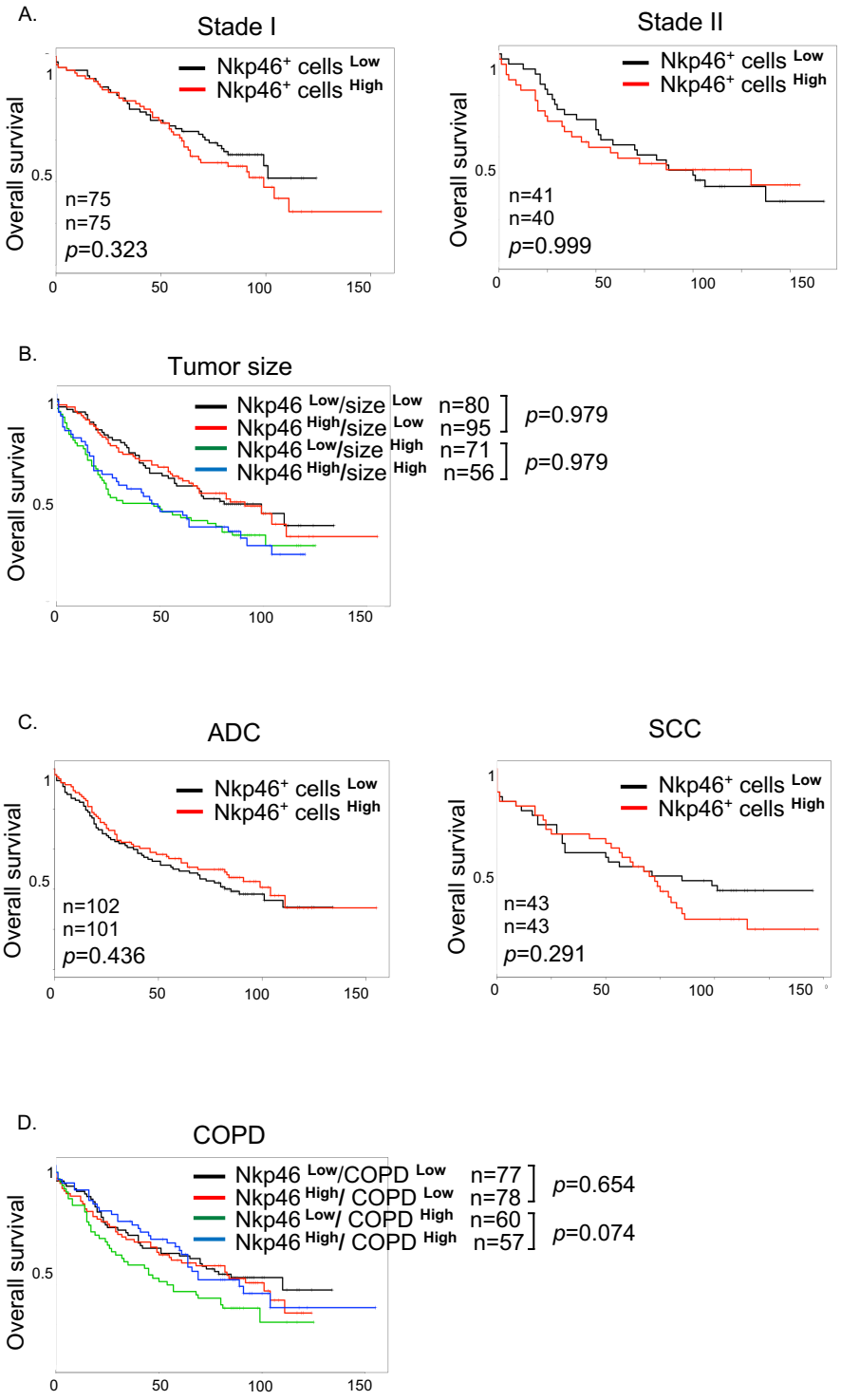
A.
Stade I
Nkp46+ cells Low
Nkp46+ cells High
Overall survival
n=75
n=75
p=0.323
Stade II
Nkp46+ cells Low
Nkp46+ cells High
n=41
n=40
p=0.999
B.
Tumor size
Nkp46 Low/size Low n=80
Nkp46 High/size Low n=95
p=0.979
Nkp46 Low/size High n=71
Nkp46 High/size High n=56
p=0.979
C.
ADC
Nkp46+ cells Low
Nkp46+ cells High
n=102
n=101
p=0.436
SCC
Nkp46+ cells Low
Nkp46+ cells High
n=43
n=43
p=0.291
D.
COPD
Nkp46 Low/COPD Low n=77
Nkp46 High/ COPD Low n=78
p=0.654
Nkp46 Low/ COPD High n=60
Nkp46 High/ COPD High n=57
p=0.074

Fig.S7

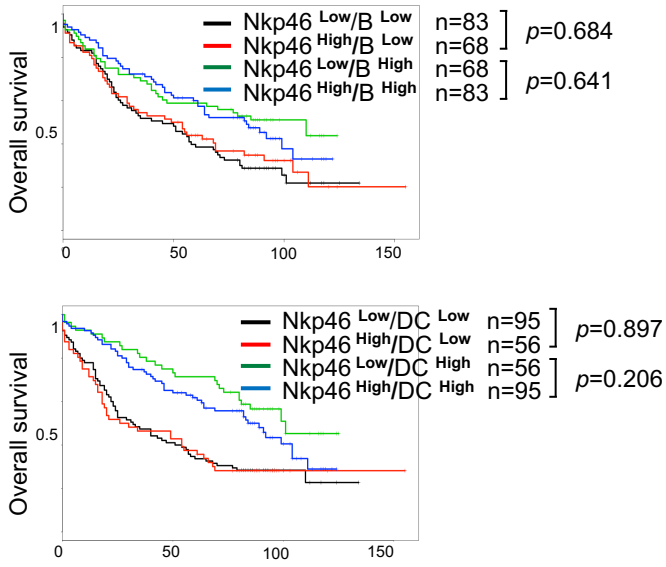
Overall survival
1
0.5
0
50
100
150
Nkp46 Low/B Low
Nkp46 High/B Low
Nkp46 Low/B High
Nkp46 High/B High
n=83
n=68
n=68
n=83
p=0.684
p=0.641
Overall survival
1
0.5
0
50
100
150
Nkp46 Low/DC Low
Nkp46 High/DC Low
Nkp46 Low/DC High
Nkp46 High/DC High
n=95
n=56
n=56
n=95
p=0.897
p=0.206

Fig.S8

A

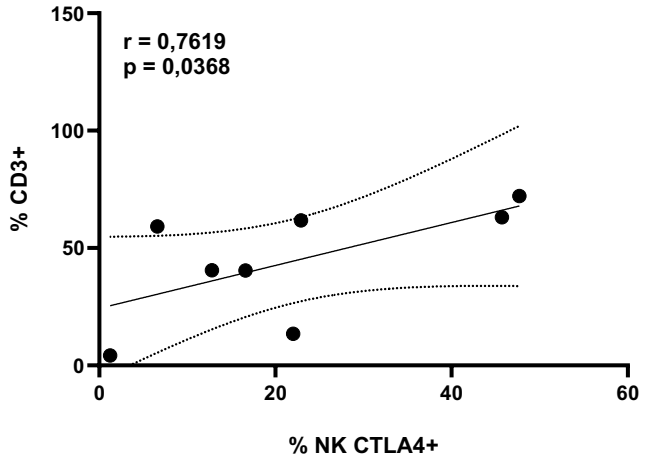
r = 0,7619
p = 0,0368
% CD3+
% NK CTLA4+
150
100
50
0
0
20
40
60

B

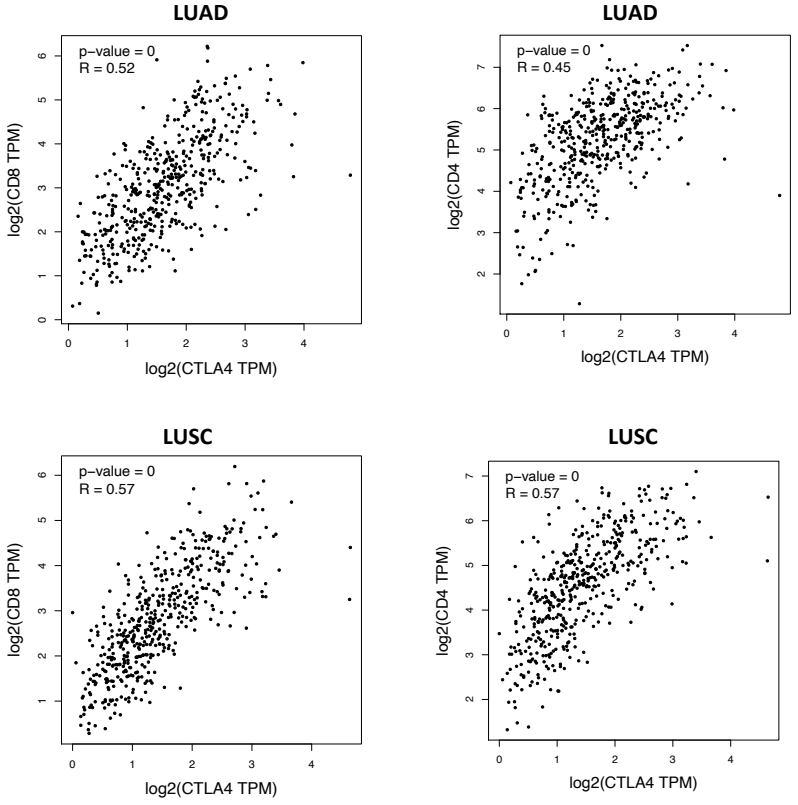
LUAD
p–value = 0
R = 0.52
log2(CD8 TPM)
log2(CTLA4 TPM)
LUAD
p–value = 0
R = 0.45
log2(CD4 TPM)
log2(CTLA4 TPM)
LUSC
p–value = 0
R = 0.57
log2(CD8 TPM)
log2(CTLA4 TPM)
LUSC
p–value = 0
R = 0.57
log2(CD4 TPM)
log2(CTLA4 TPM)

Fig.S9